The Plant Cell, Vol. 27: 1409–1427, May 2015, www.plantcell.org

HEMERA Couples the Proteolysis and Transcriptional Activity of PHYTOCHROME INTERACTING FACTORs in Arabidopsis Photomorphogenesis

Yongjian Qiu,[1] Meina Li,[1] Elise K. Pasoreck, Lingyun Long, Yiting Shi, Rafaelo M. Galvão, Conrad L. Chou, He Wang, Amanda Y. Sun, Yiyin C. Zhang, Anna Jiang, and Meng Chen[2]

Department of Biology, Duke University, Durham, North Carolina 27708

Phytochromes (phys) are red and far-red photoreceptors that control plant development and growth by promoting the proteolysis of a family of antagonistically acting basic helix-loop-helix transcription factors, the PHYTOCHROME-INTERACTING FACTORs (PIFs). We have previously shown that the degradation of PIF1 and PIF3 requires HEMERA (HMR). However, the biochemical function of HMR and the mechanism by which it mediates PIF degradation remain unclear. Here, we provide genetic evidence that HMR acts upstream of PIFs in regulating hypocotyl growth. Surprisingly, genome-wide analysis of HMR- and PIF-dependent genes reveals that HMR is also required for the transactivation of a subset of PIF direct-target genes. We show that HMR interacts with all PIFs. The HMR-PIF interaction is mediated mainly by HMR's N-terminal half and PIFs' conserved active-phytochrome B binding motif. In addition, HMR possesses an acidic nine-amino-acid transcriptional activation domain (9aaTAD) and a loss-of-function mutation in this 9aaTAD impairs the expression of PIF target genes and the destruction of PIF1 and PIF3. Together, these in vivo results support a regulatory mechanism for PIFs in which HMR is a transcriptional coactivator binding directly to PIFs and the 9aaTAD of HMR couples the degradation of PIF1 and PIF3 with the transactivation of PIF target genes.

INTRODUCTION

Light is one of the most influential environmental cues for plants, not only because it is the ultimate energy source for photosynthesis, but also because it reflects the local growth conditions as well as diurnal and seasonal time (Franklin and Quail, 2010; Kami et al., 2010). Therefore, plants have evolved a high degree of phenotypic plasticity to fine-tune their developmental programs in response to changes in environmental light cues. During seedling development, the absence or presence of light leads to morphologically distinct developmental programs. *Arabidopsis thaliana* seedlings that germinate under the ground or in the dark adopt a dark-grown developmental program called skotomorphogenesis, which promotes the elongation of the embryonic stem, or hypocotyl, and represses leaf expansion and chloroplast development. In contrast, when emerging from the ground or exposed to light, seedlings switch to a light-grown developmental program called photomorphogenesis, which restricts hypocotyl growth and promotes leaf expansion and chloroplast biogenesis (Chen and Chory, 2011). The switch to the photomorphogenetic program is driven by massive reprogramming of the transcriptome (Leivar et al., 2009). Up to one-third of Arabidopsis nuclear-encoded genes are differentially expressed between dark- and light-grown wild-type seedlings (Ma et al., 2001).

[1] These authors contributed equally to this work.
[2] Address correspondence to dr.mengchen@gmail.com.
The author responsible for distribution of materials integral to the findings presented in this article in accordance with the policy described in the Instructions for Authors (www.plantcell.org) is: Meng Chen (dr.mengchen@gmail.com).
www.plantcell.org/cgi/doi/10.1105/tpc.114.136093

Photomorphogenesis is initiated by a suite of photoreceptors, which can collectively sense the entire light spectrum ranging from UV-B to far-red light (Kami et al., 2010; Rizzini et al., 2011; Christie et al., 2012; Wu et al., 2012). Among these photoreceptors, the red (R) and far-red (FR) light-sensing phytochromes (phys) are essential for establishing photomorphogenesis (Franklin and Quail, 2010). Phys are bilin-containing proteins that can be photoconverted between two relatively stable forms: a R light-absorbing inactive Pr form and a FR light-absorbing active Pfr form (Rockwell et al., 2006; Nagatani, 2010). In Arabidopsis, phyA and phyB are the most prominent phys, and they monitor continuous FR and R light, respectively.

phys are responsible for almost the entire reprogramming of the transcriptome in response to R light (Tepperman et al., 2006; Leivar et al., 2009; Hu et al., 2013). A central mechanism by which phys initiate photomorphogenesis is by repressing the steady state levels of a family of antagonizing transcription factors called PHYTOCHROME INTERACTING FACTORs (PIFs) (Leivar and Quail, 2011; Park et al., 2012). The PIFs belong to subfamily 15 of the basic helix-loop-helix (bHLH) super protein family in Arabidopsis, which includes seven members: PIF1 and PIF3-8 (Bailey et al., 2003; Heim et al., 2003; Toledo-Ortiz et al., 2003; Leivar and Quail, 2011). All PIFs contain a C-terminal bHLH domain for DNA binding and dimerization as well as an N-terminal Active Phytochrome B binding (APB) motif, which preferentially binds to the Pfr form of phyB (Khanna et al., 2004; Leivar and Quail, 2011). PIF1 and PIF3 contain an additional Active Phytochrome A binding (APA) motif in their N termini for interacting with activated phyA (Khanna et al., 2004; Leivar and Quail, 2011). In addition to

PIFs, PHYTOCHROME INTERACTING FACTOR3-LIKE1 (PIL1), another member of subfamily 15, also contains an APB motif and can interact with phyB (Khanna et al., 2004; Luo et al., 2014). PIFs act as either transcriptional activators or repressors (Huq et al., 2004; Leivar et al., 2009, 2012; Shin et al., 2009; Toledo-Ortiz et al., 2010; Leivar and Quail, 2011; Hornitschek et al., 2012). A number of PIFs, including PIF1, PIF3, PIF4, PIF5, and PIF7, promote hypocotyl growth (Huq and Quail, 2002; Fujimori et al., 2004; Huq et al., 2004; Khanna et al., 2004; Oh et al., 2004; Al-Sady et al., 2008; Lorrain et al., 2009; Li et al., 2012). Direct-target genes induced by PIF1, 3, 4, and 5, such as *PIL1*, *ARABIDOPSIS THALIANA HOMEOBOX PROTEIN2* (*ATHB-2*), *INDOLEACETIC ACID-INDUCED PROTEIN29* (*IAA29*), and *XYLOGLUCAN ENDOTRANSGLYCOSYLASE7* (*XTR7*), encode transcription factors or enzymes involved in plant growth (Leivar et al., 2009, 2012; Oh et al., 2009, 2012; Hornitschek et al., 2012; Li et al., 2012; Zhang et al., 2013; Bernardo-García et al., 2014). PIF1, PIF3, and PIF5 also regulate nuclear-encoded genes required for chloroplast development (Huq et al., 2004; Moon et al., 2008; Leivar et al., 2009; Shin et al., 2009; Stephenson et al., 2009). Most PIFs accumulate in dark-grown seedlings, and photoactivated phys bind to PIFs and trigger their phosphorylation and subsequent degradation by ubiquitin proteasome-dependent proteolysis to initiate photomorphogenetic responses (Al-Sady et al., 2006; Lorrain et al., 2008; Shen et al., 2008; Ni et al., 2013, 2014). Consistent with this model, a quadruple *pif1 pif3 pif4 pif5* (*pifq*) mutant shows constitutive photomorphogenetic phenotypes in the dark, including a short hypocotyl and chloroplast biogenesis (Leivar et al., 2008b, 2009; Shin et al., 2009). Despite these recent advances, how phy signaling regulates the degradation of PIFs is still not fully understood.

At the subcellular level, one of the earliest light responses is the translocation of photoactivated phys from the cytoplasm to the nucleus. Within the nucleus, phys colocalize with PIFs on discrete subnuclear foci called phy speckles or photobodies (Yamaguchi et al., 1999; Kircher et al., 2002; Van Buskirk et al., 2012). The steady state pattern of phyB-GFP photobodies is directly regulated by light quality and quantity (Chen et al., 2003). The phyB-containing photobodies persist into darkness and are tightly correlated with phyB-mediated repression of PIF3 accumulation and hypocotyl growth in the dark (Rausenberger et al., 2010; Van Buskirk et al., 2014). In a genetic screen aimed at identifying factors required for the localization of phyB-GFP to photobodies, we recently uncovered a phy signaling component named HEMERA (HMR) (Chen et al., 2010b). Photoactivated phys interact directly with HMR and enhance HMR accumulation in the light to establish photomorphogenesis (Chen et al., 2010b; Galvão et al., 2012). More interestingly, HMR is required for the degradation of PIF1 and PIF3 in the light (Chen et al., 2010b; Galvão et al., 2012). However, the biochemical function of HMR and the mechanism by which HMR regulates PIF degradation remain unclear. In this study, we investigated both the genetic and mechanistic relationship between HMR and PIFs. Our study reveals an unexpected link between the degradation of PIFs and the transactivation of their target genes.

RESULTS

HMR Acts Genetically Upstream of PIFs in Regulating Hypocotyl Growth

The *hmr* mutant is impaired in both the light-mediated inhibition of hypocotyl growth and promotion of chloroplast development (Chen et al., 2010b; Chen and Chory, 2011). Because PIF1 and PIF3 fail to be degraded in the *hmr* mutant in the light (Chen et al., 2010b; Galvão et al., 2012), we asked whether the phenotypes of *hmr* depend on the accumulation of PIFs. To that end, we crossed a null *hmr* allele, *hmr-5*, with the *pifq* quadruple mutant (Leivar et al., 2008b) to generate a *hmr-5pifq* quintuple mutant. Interestingly, the long hypocotyl phenotype of *hmr-5* was largely rescued in *hmr-5pifq* seedlings (Figures 1A and 1B), indicating that the long hypocotyl phenotype of *hmr-5* is due to the accumulation of PIFs. The fact that *hmr-5 pifq* seedlings are still slightly taller than *pifq* seedlings implies that HMR might regulate other PIFs besides the four tested. Similar to the phenotypes in the light, *hmr-5 pifq* seedlings showed the same hypocotyl phenotype as *pifq* in the dark (Figures 1A and 1B), indicating that *pifq* is epistatic to *hmr-5* in regulating hypocotyl elongation. Together with our previous results that *hmr* partially represses the short hypocotyl phenotype of the constitutively active *phyB* allele, *YHB*, in the dark (Chen et al., 2010b; Galvão et al., 2012), these results indicate that HMR acts genetically between phys and PIFs in regulating hypocotyl growth.

In contrast to the hypocotyl phenotype, the albino phenotype of *hmr-5* was not rescued in *hmr-5 pifq* seedlings (Figure 1A). Similar to *hmr-5*, the *hmr-5 pifq* seedlings showed the same defects in the expression of plastid-encoded marker genes transcribed by the plastid-encoded plastid RNA polymerase (PEP) but an enhanced expression of those transcribed by the nuclear-encoded plastid RNA polymerase (Figure 1C) (Pfalz et al., 2006; Chen et al., 2010b), indicating that HMR plays a separate, PIF-independent role in PEP-mediated plastidial gene expression. This conclusion is consistent with the nuclear and plastidial dual localization of HMR and the proposed role of plastid-localized HMR, also called pTAC12, as an essential component of PEP (Pfalz et al., 2006; Chen et al., 2010b; Williams-Carrier et al., 2014). Together, these genetic data demonstrate that HMR regulates downstream photomorphogenetic responses by playing separate roles: a PIF-dependent role in regulating hypocotyl growth and a PIF-independent role in promoting chloroplast development.

HMR Is Required for the Transactivation of a Set of PIF Target Genes

PIFs act as transcriptional activators in the dark or under shade conditions to promote hypocotyl growth (Huq et al., 2004; Al-Sady et al., 2008; de Lucas et al., 2008; Shen et al., 2008; Hornitschek et al., 2009). To investigate how HMR regulates the functions of PIFs, we performed microarray analysis to examine how PIF-regulated genes are altered genome-wide in the *hmr* mutant. Our microarray analysis identified 1348 genes that were changed statistically significantly and by 2-fold between 4-d-old red-light-grown *hmr-5* and wild-type Columbia-0 (Col-0) (Supplemental Data Set 1). To determine how many

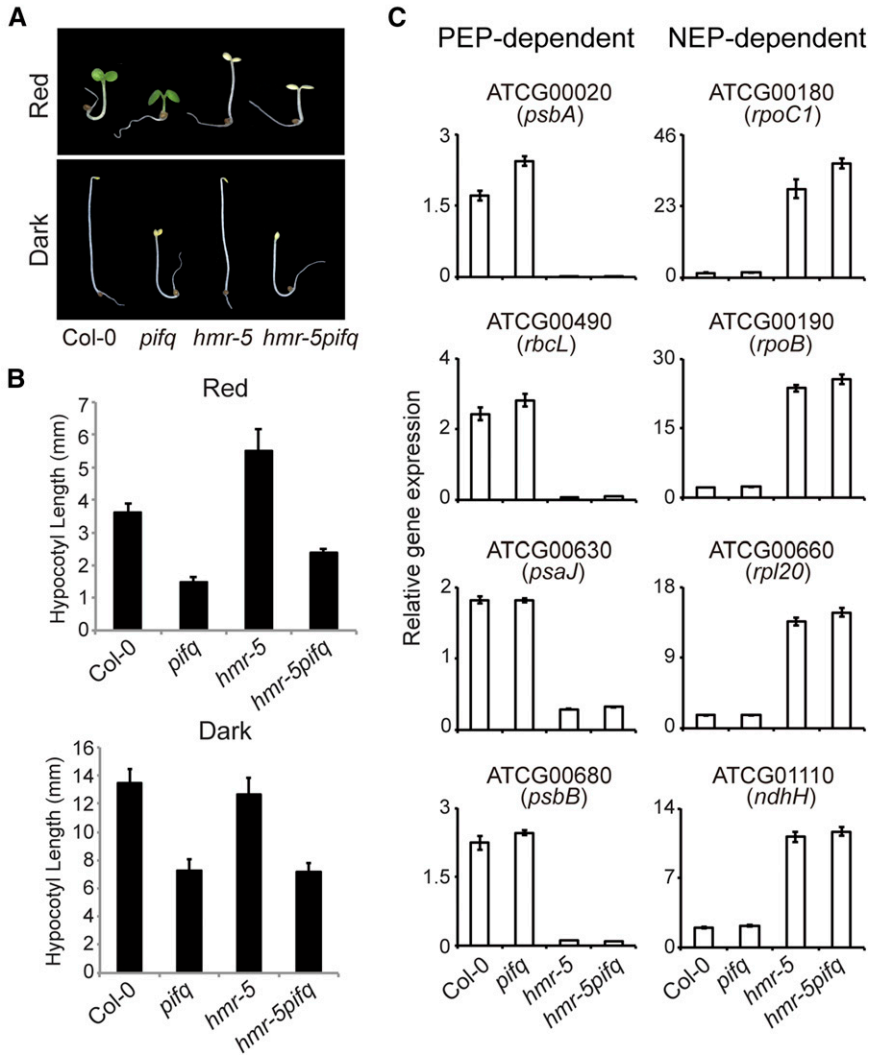

Figure 1. HMR Regulates Hypocotyl Growth and Chloroplast Biogenesis through Separate PIF-Dependent and PIF-Independent Pathways.

(A) Images of 4-d-old Col-0, *pifq*, *hmr-5*, and *hmr-5 pifq* mutants grown in 10 μmol m^{-2} s^{-1} R light (upper panel) and in the dark (lower panel).
(B) Hypocotyl measurements of the seedlings shown in **(A)**. Error bars represent standard errors.
(C) qRT-PCR analyses of the relative expression levels of representative PEP- and nuclear-encoded plastid RNA polymerase (NEP)-dependent genes in 4-d-old Col-0, *pifq*, *hmr-5*, and *hmr-5 pifq* seedlings grown in 10 μmol m^{-2} s^{-1} R light. Transcript levels were calculated relative to those of *PP2A*. Error bars represent the SD of three replicates.

HMR-dependent genes are PIF regulated, we compared the 1348 HMR-dependent genes with a previously defined set of 1028 PIF-regulated genes (Leivar et al., 2009), and we found that 203 PIF-regulated genes were significantly changed by at least twofold in *hmr-5* (Figure 2A; Supplemental Data Set 2). The 203 HMR-dependent, PIF-regulated genes include 62 PIF-induced genes and 141 PIF-repressed genes (Supplemental Data Set 2) (Leivar et al., 2009). Because the steady state levels of PIF1 and PIF3 are elevated in *hmr* mutants (Chen et al., 2010b), it was expected that PIF-induced genes would be upregulated and PIF-repressed genes downregulated in *hmr-5*. However, this was not entirely the case. While the majority of the 141 PIF-repressed genes were downregulated in *hmr-5* (Supplemental Data Set 2), surprisingly, among the 62 HMR-dependent PIF-induced genes, only 27 were upregulated in *hmr-5*; we named this group the Class A genes (Figure 2B). In contrast, more than half of the 62 HMR-dependent PIF-induced genes were downregulated (Figure 2B; Supplemental Data Set 2), indicating that the transactivation of this set of PIF-induced genes is impaired in *hmr-5*. Because the 1028 PIF-regulated genes were defined based on their expression in *pifq* mutants and Col-0, some of them might not be direct-target genes of PIFs (Leivar et al., 2009; Pfeiffer et al., 2014). Recent ChIP-seq and RNA-seq analyses have identified genes that are bound and regulated by individual PIFs or a combination of PIF1, 3, 4, and 5 (Hornitschek et al., 2012; Oh et al., 2012; Zhang et al.,

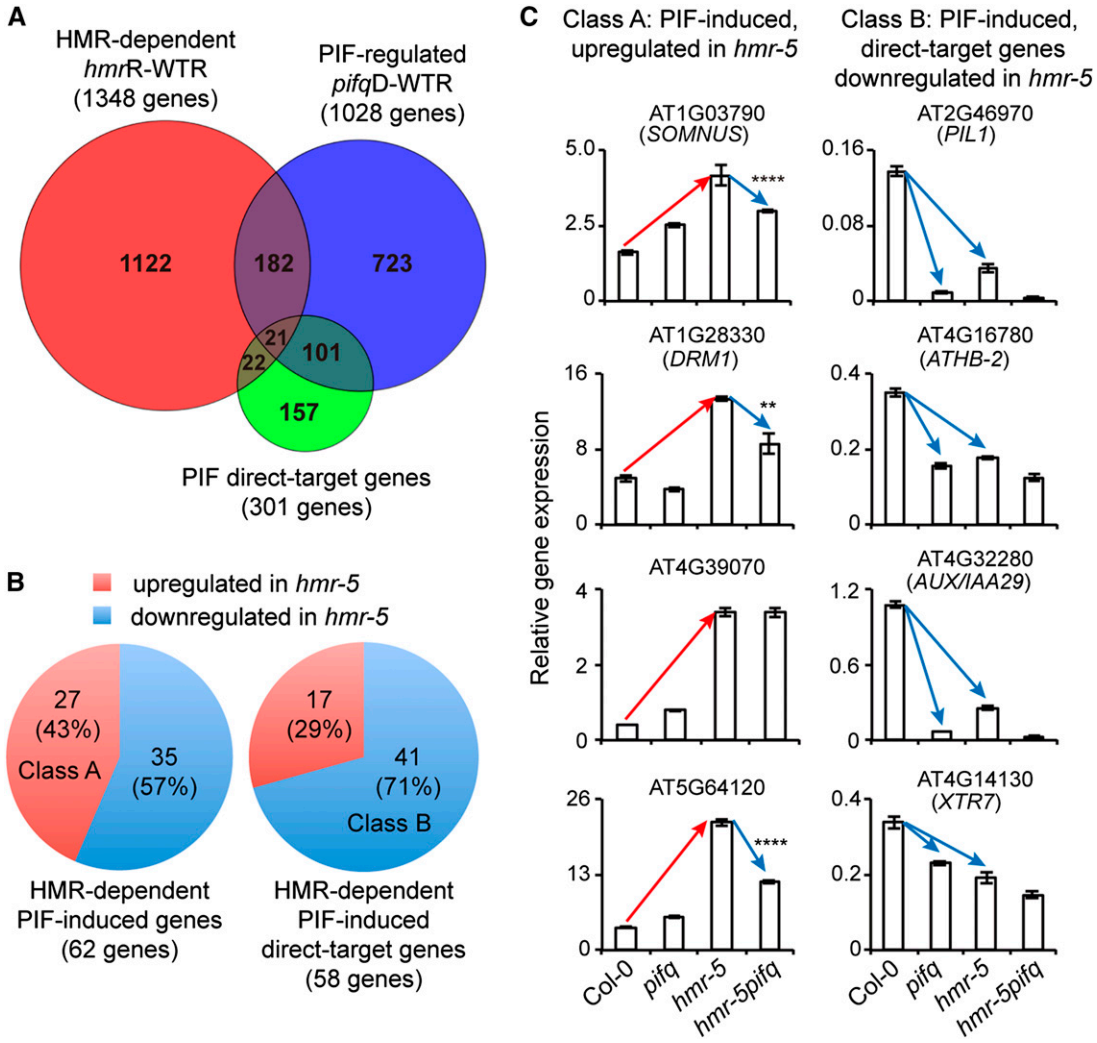

Figure 2. HMR Is Required for the Activation of a Distinct Set of PIF Target Genes.

(A) Venn diagram showing that 203 of the 1348 HMR-dependent genes overlap with the previously defined 1028 PIF-regulated genes (Leivar et al., 2009) and that 43 HMR-dependent genes belong to the 301 PIF direct-target genes (Pfeiffer et al., 2014).

(B) Pie charts showing that the majority of HMR-dependent, PIF-induced genes are downregulated in *hmr-5*. Among the 62 HMR-dependent PIF-induced genes (Supplemental Data Set 2), 27 genes (the Class A genes), or 43%, were induced in *hmr-5*; surprisingly, 57% of these genes were downregulated in *hmr-5*. Among the 58 PIF-induced direct targets that were changed statistically significantly by 1.5-fold in *hmr-5* (Supplemental Data Set 4), 41 genes (the Class B genes), or 71%, were downregulated.

(C) qRT-PCR analyses of selected PIF-induced genes in 4-d-old Col-0, *pifq*, *hmr-5*, and *hmr-5 pifq* seedlings grown in 10 μmol m^{-2} s^{-1} R light. Transcript levels were calculated relative to those of *PP2A*. Error bars represent the SD of three replicates. Red and blue arrows indicate increases and decreases in gene expression, respectively. The expression of the Class A genes in *hmr-5* was compared with that in Col-0 using Welch's two-sample *t* test. **P < 0.01 and ****P < 0.0001.

2013; Pfeiffer et al., 2014). A total of 338 genes have been recognized as PIF direct-target genes (Pfeiffer et al., 2014), among which 301 genes are represented in the Affymetrix Arabidopsis ATH1 array (Supplemental Data Set 3). To further determine whether HMR affects the transactivation of PIF direct-target genes, we analyzed the expression of these 301 PIF direct-target genes in *hmr-5* mutants. We found that 43 of them were changed statistically significantly and by 2-fold between 4-d-old red-light-grown *hmr-5* and wild-type Col-0 (Figure 2A) and that 106 genes, or 31%, of the 301 PIF direct-target genes were changed statistically significantly by 1.5-fold, which include 58 PIF-induced and 48 PIF-repressed genes and are referred to as HMR-dependent PIF direct-target genes (Supplemental Data Set 4). Strikingly, 41 genes, or 71%, of the 58 HMR-dependent PIF-induced direct-target genes were downregulated in *hmr-5* (Figure 2B), and we named these 41 genes the Class B genes. Interestingly, the Class B genes include some of the best characterized PIF direct-target genes

involved in plant growth, such as *ATHB-2*, *IAA29*, and *XTR7* (Hornitschek et al., 2012; Oh et al., 2012; Zhang et al., 2013). To confirm the microarray data, we examined the expression of eight representative PIF-regulated genes in Col-0, *hmr-5*, *pifq*, and *hmr-5 pifq* seedlings using quantitative RT-PCR (qRT-PCR). The representative genes include four Class A genes, three Class B genes, and *PIL1*, a well-characterized PIF-induced direct-target gene that is not included in the Affymetrix ATH1 microarray (Hornitschek et al., 2012; Oh et al., 2012; Zhang et al., 2013). The qRT-PCR results for the expression of the Class A and B genes in *hmr-5* and Col-0 were consistent with those from the microarray experiments (Figure 2C). In addition, the expression of *PIL1* was also downregulated in *hmr-5* mutants, indicating that *PIL1* also belongs to the Class B genes (Figure 2C). Moreover, the data show that the elevated expression of three of the four Class A genes in *hmr-5* was reversed in *hmr-5 pifq*, indicating that the upregulation of the Class A genes in *hmr-5* mutants is largely due to the accumulation of PIFs. Therefore, the long hypocotyl phenotype of *hmr-5* could be at least partially due to the upregulation of some of the Class A genes. Strikingly, the expression of the Class B genes shows similar levels of expression in *hmr-5* and *pifq* (Figure 2C), indicating that despite the enhanced steady state levels of PIF1 and PIF3 in *hmr*, they are surprisingly not transcriptionally active to induce expression of these target genes in the absence of HMR. Together, these results unexpectedly reveal that HMR plays dual and seemingly opposing roles in promoting the degradation of PIF1 and PIF3 and facilitating the transcriptional activity of PIFs to the Class B genes.

HMR's N-Terminal Half Interacts Directly with PIF1 and PIF3

To elucidate the mechanisms by which HMR regulates the stability and transcriptional activity of PIF1 and PIF3, we asked whether HMR can regulate PIFs through direct interaction. We used a previously described transgenic line expressing HA-tagged HMR (*HMR-HA*) (Galvão et al., 2012) to examine whether PIF1 and PIF3 could be coimmunoprecipitated with HMR-HA using anti-HA antibodies. The data show that both PIF1 and PIF3 can be coimmunoprecipitated with HMR-HA (Figure 3A), indicating that HMR is associated with PIF1 and PIF3 in vivo. To demonstrate that HMR interacts directly with PIF1 and PIF3, we performed glutathione *S*-transferase (GST) pull-down assays using recombinant GST-HMR to pull down in vitro-translated HA-PIF1 and HA-PIF3. These experiments show that GST-HMR, but not GST alone, can pull down HA-PIF1 and HA-PIF3 (Figure 3B). The in vitro pull-down data also show that GST-HMR interacts with HA-PIF1 more strongly than HA-PIF3, although this difference was not noticeable in the in vivo coimmunoprecipitation experiments (Figures 3A and 3B). Based on these results, we conclude that HMR interacts directly with both PIF1 and PIF3.

To map the subdomains of HMR required for PIF1 binding, we utilized HMR truncation fragments fused with GST to pull down HA-PIF1 in vitro. These experiments showed that HMR's N-terminal half (GST-HMR-N, amino acids 1 to 352), but not its C-terminal half (GST-HMR-C, amino acids 352 to 527), could pull down HA-PIF1 (Figure 3C), indicating that the N-terminal half of HMR is both required and sufficient for PIF1 binding.

The HMR-PIF1 Interaction Is Mediated by a Dimer or Oligomer Form of PIF1's APB Motif

To determine PIF1 and PIF3's subdomains that are required for their interaction with HMR, we tested the interaction between GST-HMR and a series of N-terminal deletion fragments of PIF1. These experiments indicate that the strong interaction between PIF1 and HMR requires the APB motif of PIF1 (Figure 4A). HMR also interacts weakly with PIF1's C-terminal fragment (amino acids 209 to 478), including the bHLH domain. To test whether the N-terminal halves of PIF1 and PIF3 are sufficient for binding with HMR, we used GST-HMR to pull down either PIF1 or PIF3's N termini, which contain the APA and APB motifs (Khanna et al., 2004), or their C termini, which contain the bHLH domain (Figure 4B). Surprisingly, although GST-HMR interacts strongly with full-length PIF1, its interaction with the N- and C-terminal fragments of PIF1 was substantially reduced (Figure 4B). Additionally, GST-HMR could pull down neither the N- nor the C-terminal fragments of PIF3 (Figure 4B). These data indicate that both the N- and C-terminal halves of PIF1 and PIF3 are required for the interaction with HMR. We reasoned that one possibility could be that the C-terminal fragments of PIF1 and PIF3 are required structurally for the interaction with HMR, perhaps through dimerization or oligomerization of the bHLH domain (Murre et al., 1989). Consistent with this hypothesis, when PIF1's N-terminal fragment was fused to the dimeric Gal4 DNA binding domain (DBD) (Carey et al., 1989), it regained the strong interaction with HMR, whereas fusing it to the monomeric Gal4 activation domain (GAD) did not affect HMR binding (Figure 4B). These results indicate that HMR mainly interacts with the N-terminal half of PIF1 and that this interaction requires the dimerization or oligomerization domain of PIF1's C-terminal half, likely through the bHLH domain.

To further test that the N terminus of PIF1 is responsible for its strong interaction with HMR, we took advantage of the difference in the HMR binding affinities between PIF1 and PIF3 and swapped the N- and C-terminal fragments of PIF1 and PIF3 to generate HA-tagged chimeric proteins with either PIF1's N-terminal domain fused to PIF3's C-terminal domain (HA-1N-3C) or PIF3's N-terminal domain fused to PIF1's C-terminal domain (HA-3N-1C) (Figure 4C). GST-HMR interacted strongly with HA-1N-3C but not HA-3N-1C (Figure 4C), confirming that the strong HMR-PIF1 interaction is determined by PIF1's N-terminal fragment.

We then asked which region within the PIF1 N terminus is responsible for the HMR interaction. Because the C-terminal fragment of PIF3 does not interact with HMR (Figure 4B), we fused two truncation fragments of the N-terminal half of PIF1 to PIF3's C-terminal domain, HA-1N1-3C and HA-1N2-3C, and tested their interaction with GST-HMR (Figure 4C). The data demonstrate that HA-1N2-3C, which contains the PIF1 fragment spanning amino acids 1 through 163, confers strong interaction with HMR; this region of PIF1 contains both the APA and APB motifs (Figure 4C). When the APB of PIF1 alone was fused with the C-terminal fragment of PIF3, the recombinant protein, HA-1APB-3C, also interacted strongly with GST-HMR (Figure 4C), indicating that the APB motif of PIF1 is sufficient for the interaction with HMR. The APB and APA motifs of PIFs are involved in the interaction with active forms of phyB and phyA, respectively (Khanna et al., 2004; Al-Sady et al., 2008; Shen et al., 2008). It has been shown that the

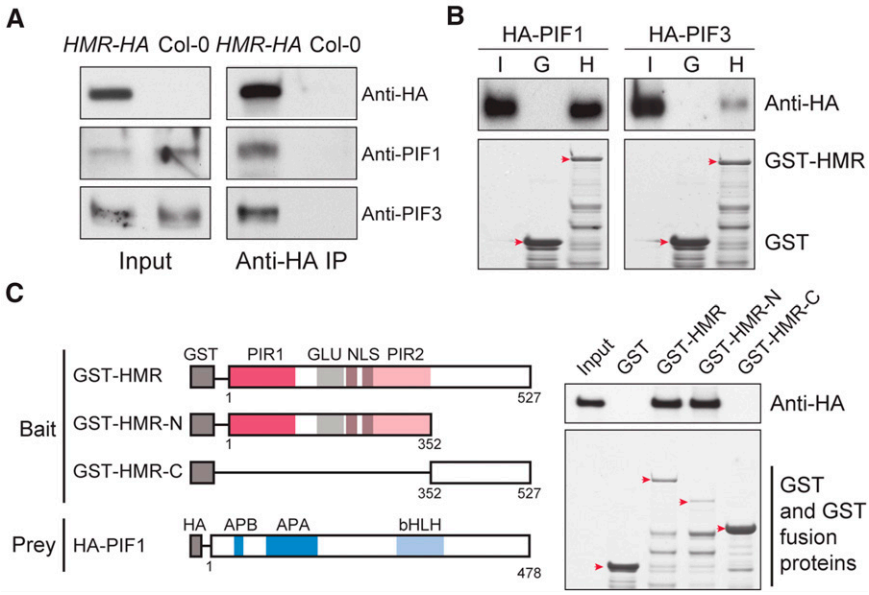

Figure 3. HMR Interacts Directly with PIF1 and PIF3 through HMR's N-Terminal Half.

(A) HMR interacts with PIF1 and PIF3 in vivo. Seedlings of the *HMR-HA* line and Col-0 were grown in 10 μmol m^{-2} s^{-1} R light for 80 h and then treated with 25 μM MG132 and 25 μM MG115 for 16 h under the same light conditions. Proteins were extracted and immunoprecipitated using anti-HA Affinity Matrix (Roche). The input and immunoprecipitated HMR-HA (top panel), PIF1 (middle panel), and PIF3 (bottom panel) were detected by immunoblots using anti-HA, anti-PIF1, and anti-PIF3 antibodies, respectively.

(B) HMR interacts directly with PIF1 and PIF3 in vitro. GST pull-down assays were performed using *Escherichia coli* expressed GST-HMR or GST to pull down in vitro-translated HA-PIF1 or HA-PIF3. HA-PIF1 and HA-PIF3 proteins were detected by immunoblots (upper panels) using anti-HA antibodies. The corresponding SDS-PAGE gels (lower panels) show the amount of GST or GST-HMR immobilized in each assay; the GST-HMR and GST bands are indicated by red arrows. GST-HMR, but not GST, was able to pull down both HA-PIF1 and HA-PIF3 in vitro. I, 10% input of HA-PIF1 or HA-PIF3; G, GST; H, GST-HMR.

(C) The N-terminal half of HMR is required and sufficient for interacting with PIF1. GST pull-down assays were performed using GST or the indicated HMR fragments fused with GST to pull down in vitro-translated HA-PIF1. The left panel shows schematics of the bait and prey proteins used in the pull-down assays. The right panel shows the results of the GST pull-down assays. Bound and 10% of input HA-PIF1 fractions were detected by immunoblot using anti-HA antibodies. Immobilized GST and GST-HMR fusion proteins are shown in the Coomassie blue-stained SDS-PAGE gel. The GST and GST-HMR fusion protein bands are indicated by red arrows. PIR1, phytochrome interacting region 1; PIR2, phytochrome interacting region 2; GLU, glutamate-rich region; NLS, nuclear localization signal.

bHLH domain is either not required for the interaction between phyB and PIFs or it attenuates this interaction (Khanna et al., 2004). Therefore, although both HMR and phyB interact with the APB motif, HMR and phyB might bind to different interfaces or distinct residues in APB. The conserved residues Glu-41 and Leu-42 in the APB of PIF1 are essential for the interaction with phyB, and mutations N144A and L95A in the APA of PIF1 abolish its interaction with phyA (Shen et al., 2008). However, mutations in these residues did not affect PIF1's interaction with HMR (Supplemental Figure 1), confirming that the HMR binding sites differ from those for phys. Taken together, these results indicate that the APB motif of PIF1 is both required and sufficient for its strong interaction with HMR. The HMR-PIF1 interaction appears to involve residues different from the phy-PIF1 interaction and require the dimerization or oligomerization function of the bHLH domain from the C-terminal half of PIF1.

HMR Interacts with All PIFs and PIL1 through the Conserved APB Motif

PIFs belong to subfamily 15 of the Arabidopsis bHLH superfamily (Toledo-Ortiz et al., 2003). Among the 15 members of subfamily 15, 12 contain an APB motif (Khanna et al., 2004). These include the seven PIFs (PIF1 and PIF3-8), PIL1, and four less-characterized bHLH proteins (bHLH127, bHLH023, bHLH119, and bHLH056) (Khanna et al., 2004). We fused the respective APB motifs from PIF3-PIF8 and PIL1 with the C-terminal fragment of PIF3 and examined their ability to bind GST-HMR using pull-down assays. The data show that GST-HMR interacts with the APB motifs from all PIFs and from PIL1 (Figure 5A). Consistent with this, GST-HMR could also pull down all full-length PIFs and PIL1 (Figure 5B). In contrast, GST-HMR failed to pull down ALCATRAZ (ALC), another subfamily 15 bHLH protein that does not contain an APB motif (Figure 5B) (Khanna et al., 2004). Together, these results demonstrate that HMR interacts directly with all PIFs and PIL1 through their conserved APB domains.

HMR Possesses an Acidic 9-Amino-Acid Transcription Activation Domain

The direct interaction between HMR and PIFs raises a hypothesis that HMR binds to PIFs to modulate their stability and activity. Because HMR is required for the activation of the Class B genes (Figure 2), one possibility is that HMR might act as

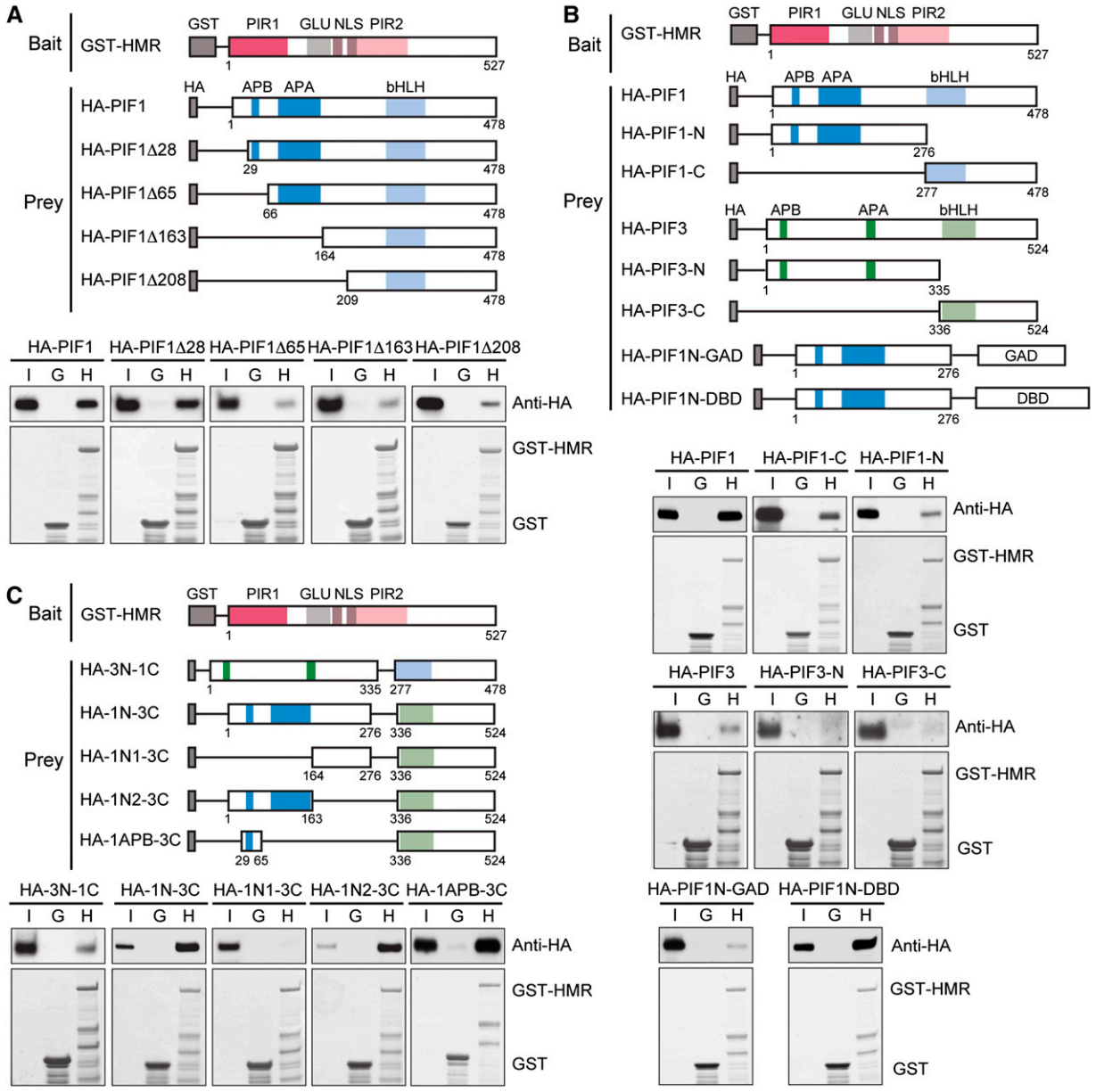

Figure 4. The HMR-PIF1 Interaction Is Mediated Mainly by PIF1's APB Motif and Requires the bHLH Dimerization Domain.

(A) The APB motif of PIF1 is required for the strong interaction with HMR. GST pull-down assays were performed using *E. coli*-expressed GST-HMR or GST to pull down in vitro-translated HA-tagged full-length PIF1 or PIF1 truncation fragments. Input and pull-down fractions of HA-tagged PIF1 fragments were detected by immunoblots using anti-HA antibodies. The corresponding SDS-PAGE gels show the amount of GST or GST-HMR immobilized in each assay. I, 10% input of the indicated PIF fragment; G, GST; H, GST-HMR; PIR1, phytochrome interacting region 1; GLU, glutamate-rich region; NLS, nuclear localization signal; PIR2, phytochrome interacting region 2; APB, active phytochrome B binding motif.

(B) HMR interacts more strongly with a dimer or oligomer form of PIF1's N-terminal half. GST pull-down assays were performed using *E. coli*-expressed GST-HMR or GST to pull down in vitro-translated HA-tagged full-length PIF1 and PIF3, the N- or C-terminal fragments of PIF1 and PIF3, and the N-terminal fragment of PIF1 fused with either Gal4 DBD or Gal4 activation domain. Input and pull-down fractions of the PIF fragments were detected by immunoblots using anti-HA antibodies. The corresponding SDS-PAGE gels show the amount of GST or GST-HMR immobilized in each assay.

(C) The APB motif of PIF1 confers the strong interaction with HMR in the presence of PIF's bHLH domain. GST pull-down assays were performed using *E. coli*-expressed GST-HMR or GST to pull down in vitro-translated HA-tagged PIF1/PIF3 chimeric proteins. Input and pull-down fractions of the PIF fragments were detected by immunoblots using anti-HA antibodies. The corresponding SDS-PAGE gels show the amount of GST or GST-HMR immobilized in each assay.

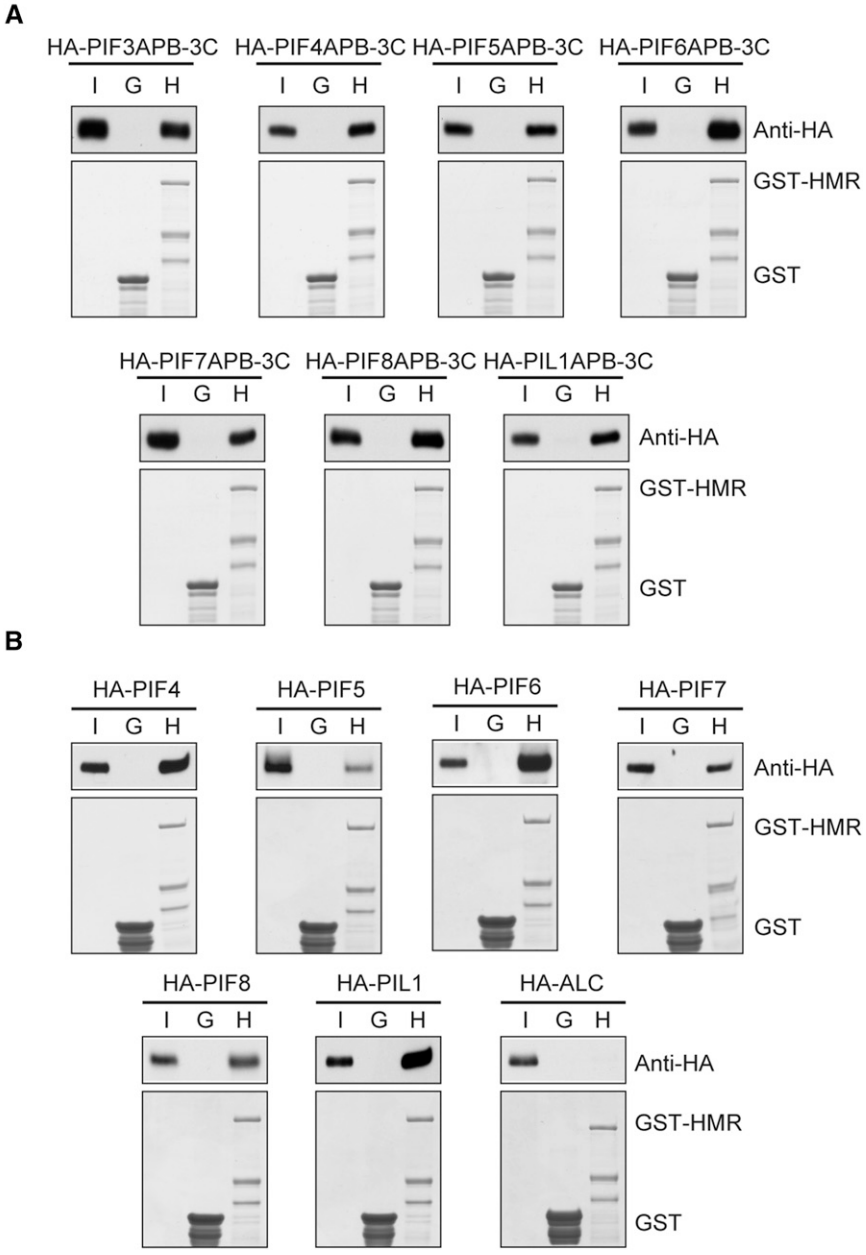

Figure 5. HMR Interacts with All PIFs and PIL1 through the Conserved APB Motif.

(A) HMR interacts with the APB motifs from all PIFs and PIL1. GST pull-down assays were performed using *E. coli*-expressed GST-HMR or GST to pull down in vitro-translated HA-tagged APB motif from indicated PIFs or PIL1 fused with the C-terminal fragment of PIF3. Input and pull-down fractions of the prey proteins were detected by immunoblots using anti-HA antibodies. The corresponding SDS-PAGE gels show the amount of GST or GST-HMR immobilized in each assay. I, 10% input of the indicated prey protein; G, GST; H, GST-HMR.

(B) HMR interacts with all PIFs and PIL1 in vitro. GST pull-down assays were performed using *E. coli*-expressed GST-HMR or GST to pull down in vitro-translated HA-tagged PIF4-8, PIL1, and ALC. Input and pull-down fractions of HA-tagged PIFs, PIL1, and ALC were detected by immunoblots using anti-HA antibodies. The corresponding SDS-PAGE gels show the amount of GST or GST-HMR immobilized in each assay.

a transcriptional coactivator. Supporting this hypothesis, full-length HMR and its C-terminal half between amino acids 254 and 527, when fused to the Gal4 DBD, were able to activate transcription in yeast (Supplemental Figure 2), suggesting that the C-terminal half of HMR contains a transcriptional activation domain. Transcriptional activation domains have been classified based on their amino acid composition into acidic, glutamine-rich, proline-rich, and serine/threonine-rich types (Mitchell and Tjian, 1989). Studies of yeast and mammalian acidic transcriptional activators have identified a nine-amino-acid transcriptional

activation domain (9aaTAD) conserved among well-characterized transcriptional activators, such as Gal4, Gcn4, Myc, and VP16 (Piskacek et al., 2007). Using the 9aaTAD prediction utility (Piskacek et al., 2007), we identified six putative 9aaTADs in the C-terminal half of HMR with match scores greater than 80% (Figure 6A). To test whether these predicted 9aaTADs function in yeast, we examined the transactivation activity of a series of truncation fragments of the C-terminal half of HMR. These experiments showed that the 9aaTAD from amino acids 512 to 520 is both required and sufficient for HMR's transactivation activity in yeast (Figure 6A). This particular 9aaTAD is highly conserved among HMR orthologs from moss to higher plants (Figure 6B). Within the 9aaTAD sequence of Arabidopsis HMR, *E*NLT*D*FLM*D*, the three acidic residues at the first, fifth, and ninth positions (italicized) are conserved among all HMR orthologs (Figure 6B). Substitutions of the conserved acidic residues individually to alanine greatly reduced the transcriptional activity of the 9aaTAD (Figure 6C). Together, these data indicate that HMR is an acidic transcriptional activator.

The Transcriptional Activity of HMR's 9aaTAD Is Required for the Activation of the Class B PIF Targets and Degradation of PIF1 and PIF3

To demonstrate the function of HMR's 9aaTAD in vivo, we employed the Seattle Arabidopsis TILLING service (http://tilling.fhcrc.org/) to search for missense mutations in the 9aaTAD (Till et al., 2003). We had previously screened for mutations in the N-terminal half of HMR and reported 11 *hmr* alleles named *hmr-4* to *hmr-14* (Supplemental Figure 3) (Galvão et al., 2012). The second round of TILLING identified eight additional missense alleles named *hmr-15* to *hmr-22* (Supplemental Figure 3). One of these alleles, *hmr*-22, carries a single amino acid substitution of the conserved acidic Asp-516 in the 9aaTAD to a noncharged Asn residue (Figure 6B). The D516N mutation reduced the transactivation activity of the 9aaTAD in yeast by 46% (Figure 6C).

To determine whether the D516N mutation affects HMR's function in phy signaling, we measured the hypocotyl growth inhibition response of *hmr-22* under a series of intensities of either R or FR light. Similar to the null *hmr-2* allele, *hmr-22* was hyposensitive to both continuous red and far-red light (Figures 7A and 7B), and it had normal cryptochrome-mediated responses in blue light (Supplemental Figure 4), indicating that *hmr-22* is impaired specifically in both phyA and phyB signaling. Seedlings of *hmr-22* are also impaired in chloroplast biogenesis (Supplemental Figure 5A). Despite the obvious defect in chloroplast development at the seedling stage, both cotyledons and leaves of *hmr-22* are able to turn green when they become fully expanded (Supplemental Figure 5B). However, the rosette of the *hmr-22* mutant is substantially smaller than that of Col-0 (Supplemental Figure 5B). Taken together, these results indicate that *hmr-22* is a weak, viable, loss-of-function *hmr* allele and that the D516N mutation attenuates HMR's functions in phy signaling and chloroplast biogenesis in vivo.

To examine the effect of the D516N mutation on the expression of the HMR-dependent PIF direct-target genes, we performed genome-wide transcriptome analysis on 4-d-old red-light-grown Col-0 and *hmr-22* seedlings using the Affymetrix ATH1 microarray. The microarray analysis identified 385 genes changed significantly by twofold between Col-0 and *hmr-22* (Supplemental Data Set 5) and 48 PIF direct-target genes were changed statistically significantly by 1.5-fold (Supplemental Data Set 6). The set of genes changed in *hmr-22* largely overlaps with those changed in *hmr-5*. Among the 385 genes changed in *hmr-22* mutants, 352 genes, or 91%, were also changed in *hmr-5* mutants (Supplemental Figure 6). Similarly, 42, or 88%, of the 48 PIF direct-target genes changed in *hmr-22* were also changed in *hmr-5* (Supplemental Figure 6). Strikingly, 21 of the 25 PIF-induced direct-target genes were downregulated in *hmr-22* mutants, including the four Class B marker genes (Figure 7C). These data indicate that the expression of the Class B PIF target genes is dependent on the transcriptional activity of HMR's 9aaTAD in vivo. Interestingly, similar to *hmr-5*, the expression of the four Class A genes was upregulated in *hmr-22* (Supplemental Figure 7), suggesting that PIF levels might also be enhanced in *hmr-22*. Indeed, PIF1 and PIF3 failed to be degraded in *hmr-22* in both R and FR light (Figure 7D). Because the D516N mutation does not alter the interaction between HMR and PIF1 in vitro (Supplemental Figure 8A), and because the level of HMR^{D516N} (HMR22) in *hmr-22* is similar to that of the wild-type HMR in Col-0 in both dark and light conditions (Supplemental Figure 8B), the defect in the degradation of PIF1 and PIF3 in *hmr-22* is most likely dependent on the activity of HMR's 9aaTAD. Together, these data indicate that HMR's 9aaTAD mediates both the degradation of PIF1 and PIF3 as well as the activation of the Class B PIF targets.

HMR Plays Dual Opposing Roles in Regulating Hypocotyl Growth

The degradation of PIF1 and PIF3 inhibits hypocotyl growth (Leivar et al., 2008b; Shin et al., 2009); in contrast, the expression of the Class B genes, including *PIL1*, *IAA29*, *ATHB2*, and *XTR7*, contributes to hypocotyl growth (Leivar et al., 2009; Hornitschek et al., 2012; Zhang et al., 2013). Therefore, HMR appears to play dual opposing roles in regulating hypocotyl growth. We hypothesize that the phenotype of *hmr* mutants should reflect a balance between these two opposing roles of HMR. We reasoned that the long hypocotyl phenotypes of *hmr* mutants in continuous R and FR light is mainly due to the accumulation of PIF1 and PIF3 because the Class B genes are expressed at low basal levels under continuous light (Leivar et al., 2009; Hornitschek et al., 2012; Zhang et al., 2013) and a further decrease in the expression of the Class B genes might not have a major impact on hypocotyl growth. Therefore, a better condition to demonstrate the physiological significance of HMR's transactivation activity is where PIF degradation is attenuated and the Class B genes are expressed at higher levels. One such condition is in the *phyB-9* background, where PIF3 degradation is impaired in the light and the four Class B genes are induced (Figures 7E and 7F) (Hornitschek et al., 2012). We then generated *hmr-22 phyB-9* double mutant. Indeed, the *hmr-22phyB-9* mutant had a similar level of PIF3 as *phyB-9* in the light (Figure 7E), confirming that the HMR-mediated PIF3 degradation is also phyB dependent. As predicted, three of the four Class B genes were downregulated in *hmr-22 phyB-9* compared with *phyB-9* (Figure 7F). More interestingly, in contrast to the long hypocotyl phenotype of *hmr-22* seedlings, the *hmr-22 phyB-9* seedlings were shorter compared with *phyB-9* seedlings (Figures 7G and 7H), indicating that the

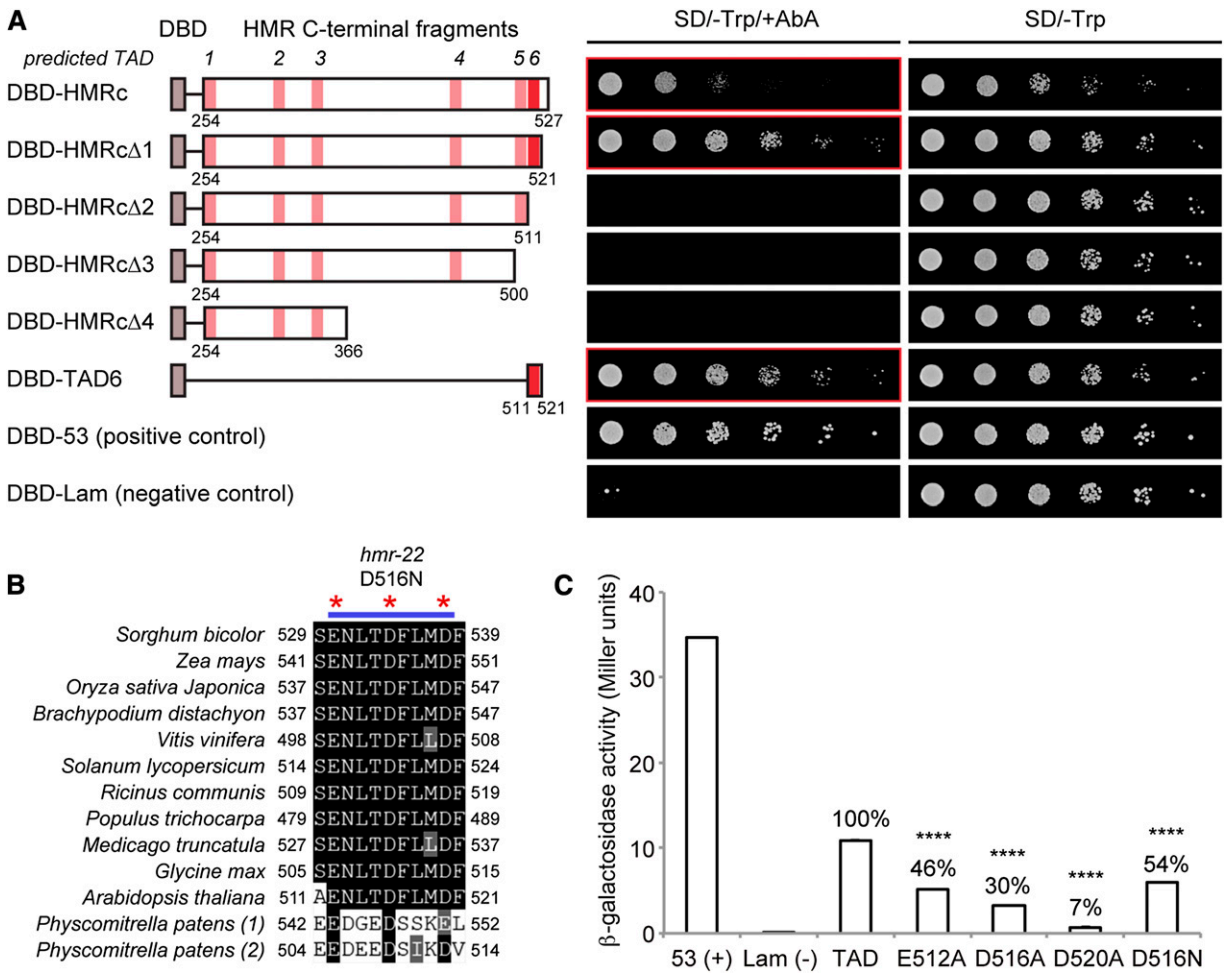

Figure 6. HMR Possesses a Conserved Acidic Nine-Amino-Acid Transactivation Domain.

(A) Dissection of the transcriptional activation domain in the C-terminal half of HMR using yeast. A series of truncation fragments of HMR's C-terminal half were fused to the GAL4 DBD in pGBKT7. The schematics of the constructs are shown in the left panel. The six predicted 9aaTADs are labeled with either pink or red blocks. TAD1, amino acids 255 to 263; TAD2, amino acids 307 to 315, TAD3, amino acids 339 to 347; TAD4, amino acids 449 to 457; TAD5, amino acids 502 to 510; and TAD6, amino acids 512 to 520. Murine p53 (53) and lamin (Lam) were used as positive and negative controls, respectively. Serial dilutions of Y2HGold (Clontech) yeast strains containing the indicated vectors were grown on either SD/-Trp or SD/-Trp/+Aureobasidin A media (right panels). Strains showing positive transactivation results are outlined with a red frame.

(B) Amino acid sequence alignment of TAD6 among HMR orthologs. The blue bar labels the 9aaTAD, and the red stars indicate the three acidic residues that are conserved among all HMR orthologs.

(C) The acidic residues of HMR's TAD are required for its full transcriptional activity in yeast. Yeast β-galactosidase liquid assays showing the transactivation activity of the wild type and mutated TADs with the indicated amino acid substitution. The D516N mutation in *hmr-22* reduces the activity of HMR's 9aaTAD by 46%. Error bars represent the standard deviations of three replicates. ****P < 0.0001.

activity of HMR's 9aaTAD is required for promoting hypocotyl growth. Together with the tall hypocotyl phenotype of *hmr* mutants, these results demonstrate that HMR plays opposing roles in regulating hypocotyl growth.

Fusion of VP16 to HMR22 Rescues Its Defects in the Transactivation of the Class B Genes but Not PIF3 Degradation

To further confirm the role of HMR in the activation of the Class B genes and to dissect the relationship between transactivation of the Class B genes and PIF degradation, we asked whether the defects of HMR22 could be rescued by fusing the transactivation domain of the Herpes simplex virus activator VP16. To this end, we generated transgenic lines expressing either HMR-HA or HMR22-HA-VP16 under the 35S promoter in *hmr-22*. We picked two independent transgenic lines for each construct for further analysis. As expected, the two *HMR-HA/hmr-22* lines (#3 and #9) rescued the long hypocotyl phenotype of *hmr-22* (Figure 8A). In contrast, the two *HMR22-HA-VP16/hmr-22* lines had even longer hypocotyls than that of *hmr-22* (Figure 8A). Both HMR-HA and HMR22-HA-VP16 were able to rescue the defects

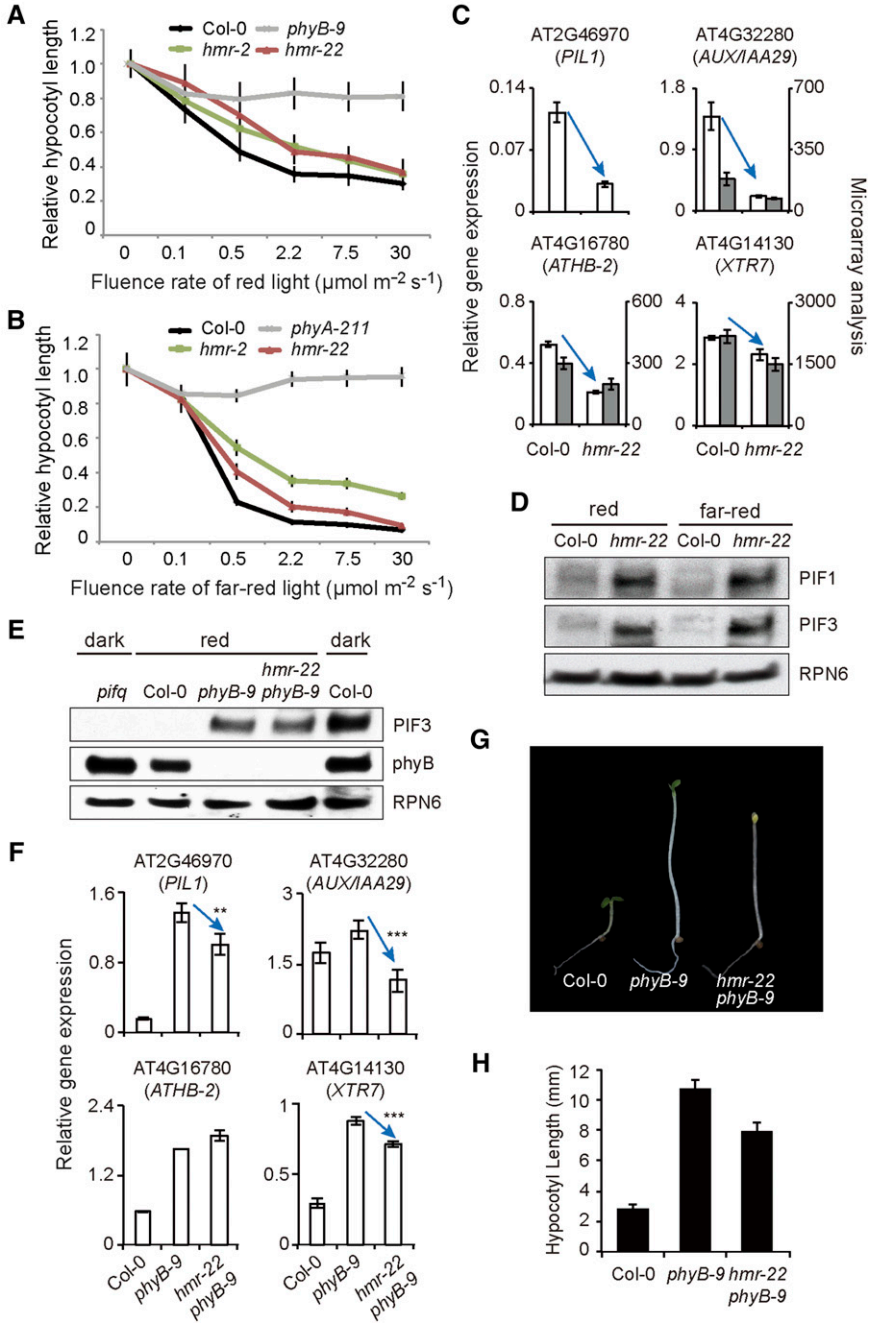

Figure 7. HMR's 9aaTAD Mediates Both the Expression of the Class B Genes and the phyB-Dependent Degradation of PIF1 and PIF3 in Vivo.

(A) Fluence response curves for R light. Relative hypocotyl length of 4-d-old Col-0, *phyB-9*, *hmr-2*, and *hmr-22* seedlings grown in various intensities of R light or in the dark.

(B) Fluence response curves for FR light. Relative hypocotyl length of 4-d-old Col-0, *phyA-211*, *hmr-2*, and *hmr-22* seedlings grown in various intensities of FR light or in the dark. Hypocotyl lengths in **(A)** and **(B)** are given relative to the average hypocotyl length of each genotype in the dark, and error bars represent standard errors from three replicates.

(C) Microarray and qRT-PCR data for the mRNA levels of the indicated PIF-induced genes in 4-d-old Col-0 and *hmr-22* seedlings grown in 10 μmol m^{-2} s^{-1} R light. In each panel, the filled columns represent data from the microarray analysis and the open columns represent confirmation data by qRT-PCR. Transcript levels from the qRT-PCR experiments were calculated relative to those of *PP2A*. Blue arrows indicate decrease in gene expression. Error bars represent the SD of three replicates.

(D) Immunoblot analysis of PIF1 and PIF3 protein levels in 4-d-old Col-0 and *hmr-22* seedlings grown in the dark, 10 μmol m^{-2} s^{-1} R light, or 10 μmol m^{-2} s^{-1} FR light. RPN6 was used as a loading control.

of *hmr-22* in the expression of the Class B genes (Figure 8B), further confirming that the activation of these PIF targets is dependent on the transactivation activity of HMR. Interestingly, whereas the *HMR-HA/hmr-22* lines rescued the defect of *hmr-22* in PIF3 degradation, the *HMR22-HA-VP16/hmr-22* lines accumulated the same level of PIF3 as *hmr-22* (Figure 8C), indicating that VP16 is not able to mediate PIF3 degradation. The combination of the elevated levels of PIF3 and the enhanced expression of the Class B genes in the *HMR22-HA-VP16/hmr-22* lines provide an explanation for their long hypocotyl phenotype (Figure 8A). Therefore, these results indicate that the degradation of PIF3 is specifically dependent on HMR's 9aaTAD. Mutations in the 9aaTAD could lead to a separation of the dual functions of HMR.

DISCUSSION

We have previously shown that the degradation of PIF1 and PIF3 in the light is dependent on HMR (Chen et al., 2010b; Galvão et al., 2012). However, the biochemical function of HMR and the mechanism by which HMR regulates PIF degradation were unclear. This study establishes the genetic and molecular functions of HMR in phy signaling. We show that *hmr-5 pifq* seedlings exhibit a similar hypocotyl phenotype as *pifq* seedlings in both light and dark conditions (Figures 1A and 1B). Combined with our previously published data that *hmr-1YHB* partially rescues the short hypocotyl phenotype of *YHB* in the dark (Galvão et al., 2012), these results indicate that HMR acts genetically between phys and PIFs in regulating hypocotyl growth. This PIF-dependent role of HMR in regulating hypocotyl growth is distinct from a PIF-independent role of HMR in plastidial gene expression and chloroplast development (Figure 1C). This study elucidates the molecular mechanism by which HMR regulates PIFs. We demonstrate that HMR is a transcriptional coactivator possessing an acidic 9aaTAD and interacting directly with all PIFs and PIL1. Surprisingly, the transactivation activity of the 9aaTAD is required for both the activation of a distinct set of growth-relevant PIF target genes, the Class B genes, including *PIL1*, *ATHB-2*, *IAA29*, and *XTR7*, as well as the degradation of PIF1 and PIF3. These in vivo data support a mechanism in which the 9aaTAD of HMR couples the degradation of PIF1 and PIF3 with the transactivation of PIF target genes (Figure 8D). We propose that HMR imposes a regulatory module to remove "spent" PIF1 and PIF3 during the transactivation of a distinct set of growth-relevant PIF target genes, and this function of HMR enables a tightly controlled mode of hypocotyl growth in the light.

HMR Is a Transcriptional Coactivator Required for the Expression of a Distinct Set of PIF Targets

The function of HMR as a transcriptional coactivator for PIF targets is first supported by the genetic evidence that despite the elevated levels of PIF1 and PIF3 in *hmr-5* mutants, the Class B PIF target genes fail to be activated (Figure 2C). Our data demonstrate that HMR is an acidic transcriptional coactivator (Figure 6) interacting directly with all PIFs and PIL1 (Figures 4 and 5). The 9aaTAD of HMR is highly conserved among HMR orthologs from various land plants, and substitutions of the conserved acidic residues in the 9aaTAD individually to alanine greatly reduced its transactivation activity in yeast (Figures 6B and 6C), indicating that the function of HMR as a transcriptional coactivator is evolutionarily conserved from moss to higher plants. The characterization of the weak allele *hmr-22*, which carries a single amino acid substitution of the conserved acidic Asp-516 in the 9aaTAD to an uncharged Asn residue, provides in vivo evidence that the transactivation activity of HMR is required for the function of HMR in phy signaling, in particular the activation of some of the Class B genes (Figures 7A to 7D). Fusion of VP16 to HMR22 rescues its defects in the transactivation of the Class B genes (Figure 8B), further confirming the conclusion that the expression of the Class B PIF targets is dependent on the transactivation activity of HMR. Consistent with these results, our previous studies have shown that although the *hmr-1YHB* double mutant had a similar level of PIF3 as the control *PBG* line in the dark, the expression of the Class B genes in *hmr-1 YHB* was much lower compared with that in *PBG* (Galvão et al., 2012), indicating that HMR is also required for the activation of these PIF targets in *YHB*.

Because expression of the Class B genes, including *PIL1*, *ATHB-2*, *IAA29*, and *XTR7*, correlates with hypocotyl growth (Leivar et al., 2009; Hornitschek et al., 2012; Zhang et al., 2013), the function of HMR in the transactivation of these genes is expected to promote hypocotyl growth. To demonstrate this function of HMR, we examined the effect of the *hmr-22* mutation in the *phyB-9* mutant, where PIF3 degradation is impaired and the expression of the Class B genes is activated (Figures 7E and 7F). The *hmr-22 phyB-9* double mutant had reduced expression of the Class B genes and hypocotyl growth compared with *phyB-9* (Figures 7E to 7H), demonstrating that the transactivation activity of HMR plays a role in promoting hypocotyl growth. This conclusion is further supported by the long hypocotyl phenotype of the *HMR22-HA-VP16/hmr-22* lines, in which the defects in the transactivation activity of HMR22 were

Figure 7. (continued).

(E) Immunoblot analysis of PIF3 protein levels in 4-d-old *phyB-9* and *hmr22 phyB9* seedlings grown in continuous 10 μmol m^{-2} s^{-1} R light. Dark-grown Col-0 and *pifq* were used as controls for the PIF3 band. RPN6 was used as a loading control.

(F) qRT-PCR data for the mRNA levels of the indicated PIF-induced genes in 4-d-old Col-0, *phyB-9*, and *hmr22 phyB-9* seedlings grown in 10 μmol m^{-2} s^{-1} R light. Transcript levels from the qRT-PCR experiments were calculated relative to those of *PP2A*. Blue arrows indicate decrease in gene expression. Error bars represent the SD of three replicates. The expression of the Class B genes in *hmr-22 phyB-9* was compared with that in *hmr-22* using Welch's two-sample *t* test. **$P < 0.01$ and ***$P < 0.001$.

(G) Representative images of 4-d-old Col-0, *phyB-9*, and *hmr22 phyB9* seedlings grown in continuous 10 μmol m^{-2} s^{-1} R light.

(H) Hypocotyl measurements of seedlings shown in **(G)**. Error bars represent standard errors.

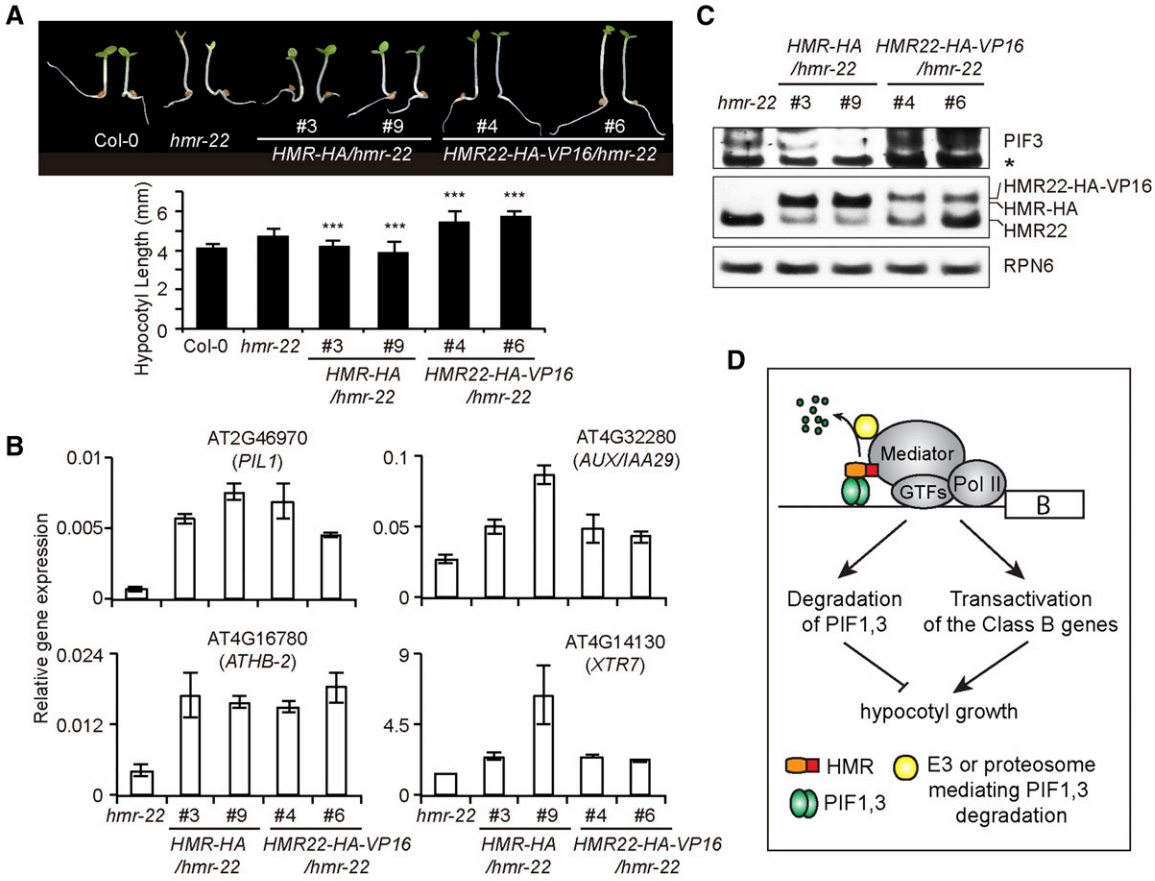

Figure 8. Fusion of VP16 to HMR22 Rescues Its Defects in Transactivation but Not in PIF3 Degradation.

(A) Images and hypocotyl measurements of 4-d-old seedlings of Col-0, *hmr-22*, and two independent transgenic lines of *HMR-HA/hmr-22* and *HMR22-HA-VP16/hmr-22* grown in continuous 10 μmol m^{-2} s^{-1} R light. Error bars represent standard error. Hypocotyls of the *HMR-HA/hmr-22* and *HMR22-HA-VP16/hmr-22* seedlings were significantly shorter or longer, respectively, than those of *hmr-22* seedlings. ***$P < 0.001$.

(B) qRT-PCR data for the mRNA levels of the indicated PIF-induced genes in 4-d-old Col-0, *hmr-22*, *HMR-HA/hmr-22*, and *HMR22-HA-VP16/hmr-22* seedlings grown in 10 μmol m^{-2} s^{-1} R light. Transcript levels from the qRT-PCR experiments were calculated relative to those of *PP2A*. Error bars represent the SD of three replicates.

(C) Immunoblot analysis of the protein levels of PIF3 and HMR in 4-d-old Col-0, *hmr-22*, *HMR-HA/hmr-22*, and *HMR22-HA-VP16/hmr-22* seedlings grown in continuous 10 μmol m^{-2} s^{-1} R light. RPN6 was used as a loading control.

(D) Proposed model for the function of HMR in regulating the stability and activity of PIF1 and PIF3. HMR binds directly to PIF1 and PIF3 on the promoters of the Class B genes. HMR's 9aaTAD mediates the transactivation of the Class B genes by recruiting and/or stabilizing the general transcriptional machinery, including general transcription factors (GTFs), the mediator complex, and the Pol II RNA polymerase. We propose that the 9aaTAD can also recruit protein degradation machineries for PIF1 and PIF3, such as E3 ubiquitin ligases or the proteasome. As such, HMR mediates the turnover of "spent" PIF1 and PIF3 during the transaction of the Class B genes. HMR enables a mechanism to tightly control hypocotyl growth by light.

rescued by VP16 but the PIF3 level remained high (Figures 8A to 8C). Together, these results show that HMR is a transcriptional coactivator binding directly to PIFs to activate the expression of the Class B PIF targets; this function of HMR promotes hypocotyl growth, which opposes the other role of HMR in mediating the degradation of PIF1 and PIF3 (Figure 8D).

How the 9aaTAD of HMR activates PIF targets is still unknown. Studies on prototypic acidic transcription activators, such as VP16, have shown that transcriptional activation domains interact directly with subunits of basal transcription factors, including TFIIA, TFIIB, TFIID, TFIIH, and subunits of the mediator complex to facilitate the assembly and/or the stability of the RNA polymerase II preinitiation complex at the transcriptional initiation site (Kobayashi et al., 1995; Uesugi et al., 1997; Hall and Struhl, 2002; Langlois et al., 2008; Borggrefe and Yue, 2011; Vojnic et al., 2011). These basic transcriptional activation mechanisms are likely conserved among eukaryotes because prototypic acidic transcriptional activation domains, such as the ones from Gal4 and VP16, are potent activators in yeast, animal, and plant cells (Ptashne, 1988; Sadowski et al., 1988; Schwechheimer et al., 1998). Consistent with this notion, this study shows that HMR's 9aaTAD is an activator in yeast and Arabidopsis (Figures 6 and 7). Therefore, HMR could work via a similar mechanism, in which HMR's N-terminal domain binds

to PIFs and the 9aaTAD at its C terminus interacts with subunits of the general transcriptional machinery (Figure 8D). Because only the expression of the Class B genes, but not the Class A genes, depends on the transcriptional activity of HMR (Figure 2C; Supplemental Figure 7), these data suggest that HMR might be associated only with the promoter regions of the Class B genes (Figure 8D). To test this model, we used the *HMR-HA* lines and examined whether the promoter regions of *PIL1*, *ATHB-2*, *IAA29*, and *XTR7* can be pulled down by HMR-HA using chromatin immunoprecipitation (ChIP). However, these ChIP experiments yielded negative results, which might be due to low efficiency of the ChIP experiments because HMR does not directly bind to DNA; alternatively, it is also possible that the PIF-HMR complex is rather unstable at the promoter regions. Further investigation is needed to distinguish these possibilities. This new model in Figure 8D also suggests that HMR might interact directly with subunits of the general transcriptional machinery. One possible candidate is the mediator subunit MED25. MED25 interacts directly with the transcriptional activation domain of VP16 (Vojnic et al., 2011). The ortholog of MED25 in Arabidopsis, known as PFT1 (Phytochrome and Flowering Time1) (Cerdán and Chory, 2003; Bäckström et al., 2007), was identified as a factor involved in phy signaling and flowering time (Cerdán and Chory, 2003; Iñigo et al., 2012a, 2012b; Klose et al., 2012). Our future investigation will test the hypothesis that HMR's 9aaTAD interacts directly with PFT1 to promote gene activation.

The 9aaTAD of HMR Mediates Both Degradation of PIF1 and PIF3 and Transactivation of PIF Targets

The current model for phy signaling suggests that phys promote the degradation of PIFs to repress the expression of PIF target genes, including the growth-relevant *PIL1*, *ATHB-2*, *IAA29*, and *XTR7* (Al-Sady et al., 2006; Ni et al., 2014). In this model, the phy-dependent degradation of PIFs serves as a restraint for the function of PIFs in promoting hypocotyl growth and degradation of PIFs is a separate process from PIF's transcriptional activity. Our results reveal an alternative mechanism, in which degradation of PIF1 and PIF3 is linked to the transactivation of the Class B PIF target genes by HMR's 9aaTAD. This counterintuitive relationship between the degradation of PIF1 and PIF3 and transactivation of PIF targets was unexpectedly revealed by our analysis of HMR-PIF-dependent genes. We found that both the degradation of PIF1 and PIF3 as well as the transactivation of the Class B PIF targets are impaired in *hmr* (Figure 2C) (Chen et al., 2010b; Galvão et al., 2012). The identification of *hmr-22*, which carries a single loss-of-function mutation in HMR's 9aaTAD (Figures 6C and 7C), allowed us to specifically test whether the transactivation activity of the 9aaTAD is required for the degradation of PIF1 and PIF3. The accumulation of PIF1 and PIF3 in *hmr-22* provides strong in vivo evidence supporting the notion that degradation of PIF1 and PIF3 is dependent on the transactivation activity of the 9aaTAD of HMR (Figure 7D). Because the level of PIF3 remained the same in *hmr-22 phyB-9* and *phyB-9* (Figure 7E), the HMR-dependent PIF3 degradation is part of the phyB-mediated mechanism of PIF3 degradation. It is intriguing that fusion of VP16 to HMR22 only rescues the defects of HMR22 in the activation of the Class B genes but not in PIF3 degradation (Figures 8B and 8C), indicating that not all transcriptional activation domains can mediate PIF degradation, there is something unique to the 9aaTAD of HMR that gives it the ability to mediate the degradation of PIF1 and PIF3.

Coupled degradation and activity has been shown for a number of prototypic unstable transcriptional activators in yeast and metazoan models, including Myc (Kim et al., 2003b; von der Lehr et al., 2003), VP16 (Salghetti et al., 2001), Gcn4 (Chi et al., 2001; Lipford et al., 2005), and the estrogen receptor (Reid et al., 2003). In fact, the transcriptional activation domains of most unstable transcription activators overlap with their degrons, the sequences for proteolysis (Muratani and Tansey, 2003). In particular, it is the acidic type, but not proline-rich or glutamine-rich, transcriptional activation domain that can mediate activator degradation (Salghetti et al., 2000). The molecular basis linking proteolysis and transcriptional activation remains elusive. However, accumulating evidence suggests that ubiquitylation and subsequent proteasome-mediated degradation of activators are an integral part of transcriptional activation (Lipford and Deshaies, 2003; Muratani and Tansey, 2003; Geng and Tansey, 2012). For example, the transcriptional activity of VP16 in yeast requires its ubiquitin ligase Met30 (Salghetti et al., 2001). In the absence of Met30, VP16 is stabilized but not transcriptionally active; fusion of ubiquitin to VP16 can bypass the requirement for Met30 for its transcriptional activity (Salghetti et al., 2001). Similarly, the transcriptional activity of the proto-oncogene Myc in human cells is dependent on Skp2, the substrate recognition subunit of a Cullin-based E3 ubiquitin ligase for Myc degradation (Kim et al., 2003b). Therefore, one possible mechanism is that the transcriptional activation domains of VP16 and Myc are required for recruiting the E3 ubiquitin ligases for their degradation. Alternatively, the ubiquitylation of activators could be required to recruit the proteasome, which has been suggested to play an important role in transcription activation besides its conventional role in protein degradation (Lipford and Deshaies, 2003; Muratani and Tansey, 2003; Geng and Tansey, 2012). Little is known about the relationship between degradation and activity of transcriptional activators in plants. However, a few lines of evidence have begun to reveal the biological importance of protein degradation in transcriptional activation in plants. First, proteasome-dependent degradation of a transcription coactivator NPR1 (Nonexpressor of Pathogenesis-Related PR genes) has been shown to stimulate the expression of pathogen responsive genes in plant immunity (Spoel et al., 2009). Second, turnover of the mediator subunit MED25 is coupled to the activation of *FLOWERING LOCUS T* in floral initiation (Iñigo et al., 2012a). Lastly, proteolysis of the transcription factor MYC2 is required for its transcriptional activity in plant immune responses (Zhai et al., 2013). Interestingly, the transcriptional activation domain of MYC2 is also an acidic type (Zhai et al., 2013). In this study, we identified another acidic transcriptional activation domain that is capable of coupling protein degradation and transcriptional activation. We propose that the mechanism of coupled degradation and activation for acidic activators is an ancient regulatory mechanism evolved prior to the divergence of the plant and animal/fungal lineages.

The 9aaTAD of HMR could work in a similar mechanism as VP16 and Myc, in which it is required to recruit either E3

ubiquitin ligases or the proteasome for the degradation of PIF1 and PIF3 during the transactivation of the Class B PIF targets (Figure 8D). Components for PIF degradation could be recruited directly by HMR or through subunits of the general transcriptional machinery (Figure 8D). In either case, PIF degradation is dependent on a unique function of HMR's 9aaTAD that is missing in VP16. It has been reported recently that the degradation of PIF3 is mediated by Cullin3-based E3 ubiquitin ligases with LRBs (Light-Response Broad-Complex/Tramtrack/Bric-a-brac) as the substrate recognition subunits (Ni et al., 2014). Interestingly, despite enhanced abundance of PIF3 in the light, the *lrb123* mutant shows a short hypocotyl phenotype (Ni et al., 2014), which resembles a *pif3* mutant as opposed to a *PIF3* overexpression line (Kim et al., 2003a; Al-Sady et al., 2008). Although it was suggested that the phenotype of *lrb123* is due to an enhanced level of phyB, an alternative explanation is that the LRB-containing E3 ubiquitin ligases are required for the function of PIF3 in vivo. These observations are consistent with our model that the ubiquitin proteasome-mediated degradation of PIF3 is coupled to the expression of PIF targets that promote hypocotyl growth. It would be interesting to investigate if HMR is involved in the ubiquitylation of PIF3 by LRBs. Another well-characterized E3 ubiquitin ligase in light signaling is COP1 (CONSTITUTIVE PHOTOMORPHOGENETIC1) (Chen et al., 2010a). Recently, COP1 has been shown to interact directly with PIF1 (Xu et al., 2014). However, because COP1 is not required for PIF3 degradation (Bauer et al., 2004), it is unlikely that COP1 is an E3 ubiquitin ligase directly regulating the activity of PIF1 and PIF3. However, further investigations are needed to examine these possibilities.

Biological Significance of the HMR-Dependent Regulation of PIF Stability and Activity

It has been proposed that linking stability and activity of transcription activators is required to remove "spent" activators and thus to tightly control transcription and downstream activator-mediated responses (Salghetti et al., 2001; Lipford and Deshaies, 2003). We suggest that the HMR-dependent PIF degradation mechanism removes "spent" PIF1 and PIF3 and enables phys to tightly control hypocotyl growth in the light (Figure 8D). It is intriguing that all prototypic unstable transcriptional activators are regulated by their own transcriptional activation domains (Muratani and Tansey, 2003), whereas PIF1 and PIF3 are regulated by the 9aaTAD of the cofactor HMR. We propose that this unique configuration of the HMR-PIF system accommodates the need to switch between two dramatically different modes of hypocotyl growth: rapid hypocotyl growth in the dark and quantitatively controlled hypocotyl growth in the light. In the dark, PIFs accumulate to high levels and the expression of the Class B genes is highly activated (Leivar et al., 2009), indicating that the degradation and activity of PIFs are uncoupled in dark-grown seedlings to maximize the speed of hypocotyl growth. Because *hmr* mutants show no obvious hypocotyl phenotype in the dark (Chen et al., 2010b) and because the level of HMR remains low in the absence of light (Galvão et al., 2012), HMR does not play a major role in hypocotyl growth the dark and HMR's 9aaTAD is likely not responsible for the expression of the Class B genes in the dark. Although the transcriptional activation domains of PIFs have not been precisely identified, PIFs have been shown to contain intrinsic transactivation activity (Huq et al., 2004; Al-Sady et al., 2008; de Lucas et al., 2008; Leivar et al., 2008a; Shen et al., 2008; Hornitschek et al., 2009). It is conceivable that the Class B genes in the dark are activated by the intrinsic transcriptional activation domains of PIFs. If this is the case, our model predicts that the intrinsic transcriptional activation domains in PIFs are not capable of coupling their degradation with their transcriptional activity. The onset of light activates the phy-mediated PIF degradation and enhances the accumulation of HMR (Al-Sady et al., 2006; Galvão et al., 2012). Binding of HMR to PIFs enables the coupling of the phyB-mediated degradation of PIF1 and PIF3 with the transactivation of the Class B PIF targets (Figure 8D). Therefore, phyB and HMR together serve as the switch to couple the stability and activity of PIF1 and PIF3 in the light, this mechanism allows hypocotyl growth to be tightly controlled in the light.

METHODS

Plant Materials, Growth Conditions, and Hypocotyl Measurement

The *hmr-1* through *hmr-14* alleles have been previously characterized (Chen et al., 2010b; Galvão et al., 2012). The ABRC accession number for the newly identified *hmr-15* to *hmr-22* alleles as well as their genotyping cleaved amplified polymorphic sequences (Konieczny and Ausubel, 1993) markers, are listed in Supplemental Table 1. All *hmr* TILLING alleles were backcrossed to Col-0 at least three times before being used for experiments. Wild-type Col-0, *phyB-9* (Col-0), and *phyA-211* (Col-0) mutants were used as controls for physiological studies. The *pifq* mutant was previously described (Leivar et al., 2008b). Seeds were surface-sterilized and plated on half-strength Murashige and Skoog growth medium without sucrose as described previously (Chen et al., 2010b). Seeds were stratified in the dark at 4°C for 5 d. Seedlings were grown at 21°C in an LED chamber (Percival Scientific) under the indicated light conditions. Fluence rates of light were measured using an Apogee PS200 spectroradiometer (Apogee Instruments).

For the measurement of hypocotyl length, seedlings were scanned using an Epson Perfection V700 photo scanner, and hypocotyls were measured using NIH ImageJ software (http://rsb.info.nih.gov/nih-image/). Data were collected from at least 30 seedlings per genotype per treatment.

Protein Extraction and Immunoblot

Protein was extracted as previously described (Shen et al., 2008) with some changes. The extraction buffer consisted of 100 mM Tris-HCl, pH 7.5, 100 mM NaCl, 5 mM EDTA, pH 8.0; 5% SDS, 20% glycerol, 20 mM DTT, 40 mM β-mercaptoethanol, 2 mM PMSF, 1× EDTA-free protease inhibitor cocktail (Roche), 80 μM MG132 (Sigma-Aldrich), 80 μM MG115 (Sigma-Aldrich), 1% phosphatase inhibitor cocktail 3 (Sigma-Aldrich), and 10 mM *N*-ethylmaleimide. Seedlings were ground directly in extraction buffer in a 1:2 (mg/μL) ratio in dim green light, boiled for 10 min, and then centrifuged at 15,000*g* for 10 min at room temperature. The supernatant was then saved for further analysis.

For immunoblots, proteins were separated on an SDS-PAGE mini-gel, transferred onto a nitrocellulose membrane, probed with the indicated primary antibodies, and then incubated with secondary goat anti-rabbit or anti-mouse antibodies (Bio-Rad) conjugated with horseradish peroxidase. The signals were detected with a chemiluminescence reaction using a SuperSignal kit (Pierce). Polyclonal anti-HMR antibodies were used at 1:500 dilution. Polyclonal anti-RPN6 antibodies (Enzo Life Sciences) were used at 1:1000 dilution. Monoclonal anti-phyB antibodies were used at

1:1000 dilution. Polyclonal anti-PIF1 and anti-PIF3 antibodies were used at 1:500 dilution.

RNA Extraction and qRT-PCR

Total RNA from seedlings of the indicated genotypes and growth conditions was isolated using the Spectrum Plant Total RNA kit (Sigma-Aldrich) with on-column DNase I (Sigma-Aldrich) treatment. cDNA was synthesized using an Invitrogen Superscript II First-Strand cDNA synthesis kit according to the manufacturer's recommendations. Oligo(dT) primers were used for the analysis of nuclear gene expression, and a mixture of oligo(dT) and gene-specific primers was used for the analysis of plastidial genes. qRT-PCR was performed with FastStart Universal SYBR Green Master Mix (Roche). All primers used are listed in Supplemental Tables 2 and 3.

Microarray Analysis

Col-0, *hmr-5*, and *hmr-22* mutant seedlings were grown in continuous red light (10 μmol m^{-2} s^{-1}) for 4 d before harvesting. Total RNA isolation was performed as described above. Three different biological replicates of each genotype were grown and sampled separately, and extracted and processed independently. Total RNA was assessed for quality with an Agilent 2100 Bioanalyzer G2939A (Agilent Technologies) and a Nanodrop 8000 spectrophotometer (Thermo Scientific/Nanodrop). Hybridization targets were prepared with a MessageAmp Premier RNA amplification kit (Applied Biosystems/Ambion) from total RNA, hybridized to GeneChip ATH1 Genome arrays in an Affymetrix 645 GeneChip hybridization oven, washed in an Affymetrix GeneChip Fluidics Station 450, and scanned with an Affymetrix GeneChip Scanner 7G according to standard Affymetrix GeneChip hybridization, wash, and stain protocols.

The microarray data analysis was performed using GeneSpring GX version software 12.1 (Agilent Technologies). The *cel* files were normalized using robust multiarray average background correction method. The Filter on Volcano plot was applied for the pairwise comparisons between Col-0 and the *hmr* mutants. Significantly differentially expressed genes were selected with the following thresholds: corrected P value < 0.05 (adjusted with Benjamini-Hochberg false discovery rate) and absolute fold change ≥ 1.5 or 2.0.

Coimmunoprecipitation

Coimmunoprecipitation experiments were performed as previously described (Chen et al., 2010b; Galvão et al., 2012) with minor modifications. Briefly, *HMR-HA* overexpression lines and Col-0 seedlings were grown in continuous red light (10 μmol m^{-2} s^{-1}) for 80 h, followed by a 16-h treatment of 25 μM MG132 and 25 μM MG115 in the same light condition. Five hundred milligrams of treated seedlings was collected and ground in liquid N_2, and the powder was resuspended in 1 mL of coimmunoprecipitation buffer containing 50 mM Tris-HCl, pH 7.5, 100 mM NaCl, 1 mM EDTA, 2 mM DTT, and 0.1% Nonidet P-40, supplemented with 40 μM MG132, 40 μM MG115, and 1× EDTA-free protease inhibitor cocktail (Roche). The crude extract was cleared by centrifugation at 20,000*g* for 2 × 10 min at 4°C. An aliquot of 0.9 mL of the cleared extract was mixed with 100 μL of anti-HA Affinity Matrix (Roche) and incubated at 4°C for 4 h. The beads were washed four times with 1 mL coimmunoprecipitation buffer, and the immunoprecipitated proteins were eluted by boiling the beads in 1× Laemmli protein sample buffer. Protein samples were subjected to 8% SDS-PAGE and the input and immunoprecipitated HMR-HA, PIF1, and PIF3 were detected by immunoblots with mouse anti-HA monoclonal (Invitrogen), rabbit anti-PIF1, and rabbit anti-PIF3 polyclonal antibodies (Chen et al., 2010b) as indicated.

GST Pull-Down

GST pull-down assays were performed as described previously (Chen et al., 2010b; Galvão et al., 2012). Briefly, GST fusion proteins were expressed in *Escherichia coli* strain BL21(DE3) host strains (Agilent Technologies) carrying pET42b vectors (Novagen). After harvesting by centrifugation at 5000*g* for 10 min at 4°C, the cells were lysed by French press in E buffer containing 50 mM Tris-HCl, pH 7.5, 100 mM NaCl, 1 mM EDTA, 1 mM EGTA, 1% DMSO, 2 mM DTT, and protease inhibitor cocktail (Sigma-Aldrich). The cell extract was prepared by centrifugation at 10,000*g* for 20 min at 4°C, followed by ultracentrifugation at 50,000*g* for 15 min at 4°C. The cleared cell extract was incubated with glutathione Sepharose beads (GE Healthcare) equilibrated in E buffer at 4°C for 2 h. The beads with the immobilized GST fusion proteins were washed four times with E buffer supplemented with 0.1% Nonidet P-40.

Prey proteins with a single N-terminal HA tag were synthesized using plasmid pCMX-PL2 and the TNT T7 Coupled Reticulocyte Lysate System (Promega) according to the manufacturer's protocol. The in vitro-translated prey proteins were diluted with E buffer supplemented with 0.1% Nonidet P-40 and incubated with the affinity-purified GST fusion protein immobilized on the beads at 4°C for 2 h. Then, the beads were washed four times with E buffer supplemented with 0.1% Nonidet P-40. Bound proteins were eluted by boiling in 1× Laemmli protein sample buffer and subjected to 8% SDS-PAGE. Input and immunoprecipitated prey proteins were detected by immunoblots using goat anti-HA polyclonal antibodies (GenScript). The amount of GST fusion proteins used in each pull-down assay was visualized by staining the SDS-PAGE with Coomassie Brilliant Blue. All primers for making the constructs used in the GST pull-down experiments are listed in Supplemental Table 4.

Yeast Transactivation Assay

Fragments of the HMR coding sequence were cloned into pGBKT7 vector and subsequently transformed into Y2HGold yeast (Clontech). Overnight yeast cultures were first diluted to an OD_{600} of 0.2, from which 5-fold serial dilutions were spotted on SD/-Trp and SD/-Trp/+Aureobasidin A. The plates were incubated at 30°C, and pictures were taken on the third day. For liquid culture assay, healthy colonies were selected and mated with yeast strain Y187 containing pGADT7 vector (Clontech). The mated diploids were cultured in SD/-Leu/-Trp media, and the transactivation assay was performed using ortho-nitrophenyl-β-galactoside as a substrate according to the Yeast Protocols Handbook (Clontech). The activity of β-galactosidase was calculated in Miller units from three replicates. Primers used to make the constructs for the yeast transactivation assays are listed in Supplemental Table 5. The wild-type and mutant versions of HMR's 9aaTAD (E512A, D516A, D516N, and D520A) were cloned into pGBKT7 vector and transformed into Y2HGold. The primers used to make these constructs are listed in Supplemental Table 6.

Accession Numbers

Sequence data from this article can be found in the Arabidopsis Genome Initiative or GenBank/EMBL databases under the accession numbers listed in Supplemental Tables 2 and 3.

Supplemental Data

Supplemental Figure 1. Residues in the APB and APA essential for phyB or phyA interaction are not required for the interaction with HMR.

Supplemental Figure 2. The C-terminal half of HMR possesses transactivation activity in yeast.

Supplemental Figure 3. The *hmr* allele collection.

Supplemental Figure 4. *hmr-22* has a normal hypocotyl growth response in blue light.

Supplemental Figure 5. *hmr-22* is a weak, viable allele of *hmr*.

Supplemental Figure 6. A similar set of genes was misregulated in *hmr-22* and *hmr-5*.

Supplemental Figure 7. The expression of the Class A HMR-PIF-dependent genes is upregulated in *hmr-22*.

Supplemental Figure 8. A D516N mutation in HMR22 affects neither the affinity of HMR to PIF1 in vitro nor HMR's accumulation in vivo.

Supplemental Table 1. CAPS markers for genotyping *hmr-14* to *-22* mutants.

Supplemental Table 2. qRT-PCR primers for the nuclear-encoded genes examined in this study.

Supplemental Table 3. Primers used to measure the transcript levels of plastidial-encoded genes.

Supplemental Table 4. Primers used for making the bait and prey constructs for the GST pull-down assays.

Supplemental Table 5. Primers used to amplify HMR fragments for the constructs used in the yeast transactivation assays.

Supplemental Table 6. Primers used to introduce single amino acid substitutions in HMR's 9aaTAD.

Supplemental Data Set 1. HMR-dependent genes in continuous R light.

Supplemental Data Set 2. HMR-PIF-dependent genes.

Supplemental Data Set 3. A list of 301 PIF direct-target genes represented in the Affymetrix ATH1 array.

Supplemental Data Set 4. HMR-dependent PIF direct-target genes.

Supplemental Data Set 5. Genes changed statistically significantly and by twofold in *hmr-22*.

Supplemental Data Set 6. PIF direct-target genes changed in *hmr-22*.

ACKNOWLEDGMENTS

We thank Chan Yul Yoo and P. Andrew Nevarez for their critical comments and suggestions regarding this article. This work was supported by grants from the National Institutes of Health (R01GM087388) and the National Science Foundation (IOS-1051602) to M.C. Y.S. was supported by a fellowship from the Chinese International Postdoctoral Exchange Program. M.C. expresses his deepest gratitude to Tai-ping Sun and Zhenming Pei for their kind support and encouragement during the treacherous time when this article was being prepared.

AUTHOR CONTRIBUTIONS

Y.Q., M.L., E.K.P., and M.C. designed the research. Y.Q., M.L., E.K.P., L.L., Y.S., R.M.G., H.W., C.L.C., A.Y.S., Y.C.Z., A.J., and M.C. performed research. Y.Q., M.L., E.K.P., R.M.G., and M.C. analyzed data. Y.Q., M.L., E.K.P., and M.C. wrote the article.

Received December 30, 2014; revised March 25, 2015; accepted April 10, 2015; published May 5, 2015.

REFERENCES

Al-Sady, B., Kikis, E.A., Monte, E., and Quail, P.H. (2008). Mechanistic duality of transcription factor function in phytochrome signaling. Proc. Natl. Acad. Sci. USA **105:** 2232–2237.

Al-Sady, B., Ni, W., Kircher, S., Schäfer, E., and Quail, P.H. (2006). Photoactivated phytochrome induces rapid PIF3 phosphorylation prior to proteasome-mediated degradation. Mol. Cell **23:** 439–446.

Bäckström, S., Elfving, N., Nilsson, R., Wingsle, G., and Björklund, S. (2007). Purification of a plant mediator from *Arabidopsis thaliana* identifies PFT1 as the Med25 subunit. Mol. Cell **26:** 717–729.

Bailey, P.C., Martin, C., Toledo-Ortiz, G., Quail, P.H., Huq, E., Heim, M.A., Jakoby, M., Werber, M., and Weisshaar, B. (2003). Update on the basic helix-loop-helix transcription factor gene family in *Arabidopsis thaliana.* Plant Cell **15:** 2497–2502.

Bauer, D., Viczián, A., Kircher, S., Nobis, T., Nitschke, R., Kunkel, T., Panigrahi, K.C., Adám, E., Fejes, E., Schäfer, E., and Nagy, F. (2004). Constitutive photomorphogenesis 1 and multiple photoreceptors control degradation of phytochrome interacting factor 3, a transcription factor required for light signaling in *Arabidopsis.* Plant Cell **16:** 1433–1445.

Bernardo-García, S., de Lucas, M., Martínez, C., Espinosa-Ruiz, A., Davière, J.M., and Prat, S. (2014). BR-dependent phosphorylation modulates PIF4 transcriptional activity and shapes diurnal hypocotyl growth. Genes Dev. **28:** 1681–1694.

Borggrefe, T., and Yue, X. (2011). Interactions between subunits of the Mediator complex with gene-specific transcription factors. Semin. Cell Dev. Biol. **22:** 759–768.

Carey, M., Kakidani, H., Leatherwood, J., Mostashari, F., and Ptashne, M. (1989). An amino-terminal fragment of GAL4 binds DNA as a dimer. J. Mol. Biol. **209:** 423–432.

Cerdán, P.D., and Chory, J. (2003). Regulation of flowering time by light quality. Nature **423:** 881–885.

Chen, H., Huang, X., Gusmaroli, G., Terzaghi, W., Lau, O.S., Yanagawa, Y., Zhang, Y., Li, J., Lee, J.H., Zhu, D., and Deng, X.W. (2010a). *Arabidopsis* CULLIN4-damaged DNA binding protein 1 interacts with CONSTITUTIVELY PHOTOMORPHOGENIC1-SUPPRESSOR OF PHYA complexes to regulate photomorphogenesis and flowering time. Plant Cell **22:** 108–123.

Chen, M., and Chory, J. (2011). Phytochrome signaling mechanisms and the control of plant development. Trends Cell Biol. **21:** 664–671.

Chen, M., Schwab, R., and Chory, J. (2003). Characterization of the requirements for localization of phytochrome B to nuclear bodies. Proc. Natl. Acad. Sci. USA **100:** 14493–14498.

Chen, M., Galvão, R.M., Li, M., Burger, B., Bugea, J., Bolado, J., and Chory, J. (2010b). *Arabidopsis* HEMERA/pTAC12 initiates photomorphogenesis by phytochromes. Cell **141:** 1230–1240.

Chi, Y., Huddleston, M.J., Zhang, X., Young, R.A., Annan, R.S., Carr, S.A., and Deshaies, R.J. (2001). Negative regulation of Gcn4 and Msn2 transcription factors by Srb10 cyclin-dependent kinase. Genes Dev. **15:** 1078–1092.

Christie, J.M., Arvai, A.S., Baxter, K.J., Heilmann, M., Pratt, A.J., O'Hara, A., Kelly, S.M., Hothorn, M., Smith, B.O., Hitomi, K., Jenkins, G.I., and Getzoff, E.D. (2012). Plant UVR8 photoreceptor senses UV-B by tryptophan-mediated disruption of cross-dimer salt bridges. Science **335:** 1492–1496.

de Lucas, M., Davière, J.M., Rodríguez-Falcón, M., Pontin, M., Iglesias-Pedraz, J.M., Lorrain, S., Fankhauser, C., Blázquez, M.A., Titarenko, E., and Prat, S. (2008). A molecular framework for light and gibberellin control of cell elongation. Nature **451:** 480–484.

Franklin, K.A., and Quail, P.H. (2010). Phytochrome functions in *Arabidopsis* development. J. Exp. Bot. **61:** 11–24.

Fujimori, T., Yamashino, T., Kato, T., and Mizuno, T. (2004). Circadian-controlled basic/helix-loop-helix factor, PIL6, implicated in light-signal transduction in *Arabidopsis thaliana.* Plant Cell Physiol. **45:** 1078–1086.

Galvão, R.M., Li, M., Kothadia, S.M., Haskel, J.D., Decker, P.V., Van Buskirk, E.K., and Chen, M. (2012). Photoactivated phytochromes interact with HEMERA and promote its accumulation to establish photomorphogenesis in Arabidopsis. Genes Dev. **26:** 1851–1863.

Geng, F., and Tansey, W.P. (2012). Similar temporal and spatial recruitment of native 19S and 20S proteasome subunits to transcriptionally active chromatin. Proc. Natl. Acad. Sci. USA **109:** 6060–6065.

Hall, D.B., and Struhl, K. (2002). The VP16 activation domain interacts with multiple transcriptional components as determined by protein-protein cross-linking in vivo. J. Biol. Chem. **277:** 46043–46050.

Heim, M.A., Jakoby, M., Werber, M., Martin, C., Weisshaar, B., and Bailey, P.C. (2003). The basic helix-loop-helix transcription factor family in plants: a genome-wide study of protein structure and functional diversity. Mol. Biol. Evol. **20:** 735–747.

Hornitschek, P., Lorrain, S., Zoete, V., Michielin, O., and Fankhauser, C. (2009). Inhibition of the shade avoidance response by formation of non-DNA binding bHLH heterodimers. EMBO J. **28:** 3893–3902.

Hornitschek, P., Kohnen, M.V., Lorrain, S., Rougemont, J., Ljung, K., López-Vidriero, I., Franco-Zorrilla, J.M., Solano, R., Trevisan, M., Pradervand, S., Xenarios, I., and Fankhauser, C. (2012). Phytochrome interacting factors 4 and 5 control seedling growth in changing light conditions by directly controlling auxin signaling. Plant J. **71:** 699–711.

Hu, W., Franklin, K.A., Sharrock, R.A., Jones, M.A., Harmer, S.L., and Lagarias, J.C. (2013). Unanticipated regulatory roles for *Arabidopsis* phytochromes revealed by null mutant analysis. Proc. Natl. Acad. Sci. USA **110:** 1542–1547.

Huq, E., and Quail, P.H. (2002). PIF4, a phytochrome-interacting bHLH factor, functions as a negative regulator of phytochrome B signaling in *Arabidopsis.* EMBO J. **21:** 2441–2450.

Huq, E., Al-Sady, B., Hudson, M., Kim, C., Apel, K., and Quail, P.H. (2004). Phytochrome-interacting factor 1 is a critical bHLH regulator of chlorophyll biosynthesis. Science **305:** 1937–1941.

Iñigo, S., Giraldez, A.N., Chory, J., and Cerdán, P.D. (2012a). Proteasome-mediated turnover of *Arabidopsis* MED25 is coupled to the activation of FLOWERING LOCUS T transcription. Plant Physiol. **160:** 1662–1673.

Iñigo, S., Alvarez, M.J., Strasser, B., Califano, A., and Cerdán, P.D. (2012b). PFT1, the MED25 subunit of the plant Mediator complex, promotes flowering through CONSTANS dependent and independent mechanisms in *Arabidopsis.* Plant J. **69:** 601–612.

Kami, C., Lorrain, S., Hornitschek, P., and Fankhauser, C. (2010). Light-regulated plant growth and development. Curr. Top. Dev. Biol. **91:** 29–66.

Khanna, R., Huq, E., Kikis, E.A., Al-Sady, B., Lanzatella, C., and Quail, P.H. (2004). A novel molecular recognition motif necessary for targeting photoactivated phytochrome signaling to specific basic helix-loop-helix transcription factors. Plant Cell **16:** 3033–3044.

Kim, J., Yi, H., Choi, G., Shin, B., Song, P.S., and Choi, G. (2003a). Functional characterization of phytochrome interacting factor 3 in phytochrome-mediated light signal transduction. Plant Cell **15:** 2399–2407.

Kim, S.Y., Herbst, A., Tworkowski, K.A., Salghetti, S.E., and Tansey, W.P. (2003b). Skp2 regulates Myc protein stability and activity. Mol. Cell **11:** 1177–1188.

Kircher, S., Gil, P., Kozma-Bognár, L., Fejes, E., Speth, V., Husselstein-Muller, T., Bauer, D., Adám, E., Schäfer, E., and Nagy, F. (2002). Nucleocytoplasmic partitioning of the plant photoreceptors phytochrome A, B, C, D, and E is regulated differentially by light and exhibits a diurnal rhythm. Plant Cell **14:** 1541–1555.

Klose, C., Büche, C., Fernandez, A.P., Schäfer, E., Zwick, E., and Kretsch, T. (2012). The mediator complex subunit PFT1 interferes with COP1 and HY5 in the regulation of *Arabidopsis* light signaling. Plant Physiol. **160:** 289–307.

Kobayashi, N., Boyer, T.G., and Berk, A.J. (1995). A class of activation domains interacts directly with TFIIA and stimulates TFIIA-TFIID-promoter complex assembly. Mol. Cell. Biol. **15:** 6465–6473.

Konieczny, A., and Ausubel, F.M. (1993). A procedure for mapping *Arabidopsis* mutations using co-dominant ecotype-specific PCR-based markers. Plant J. **4:** 403–410.

Langlois, C., Mas, C., Di Lello, P., Jenkins, L.M., Legault, P., and Omichinski, J.G. (2008). NMR structure of the complex between the Tfb1 subunit of TFIIH and the activation domain of VP16: structural similarities between VP16 and p53. J. Am. Chem. Soc. **130:** 10596–10604.

Leivar, P., and Quail, P.H. (2011). PIFs: pivotal components in a cellular signaling hub. Trends Plant Sci. **16:** 19–28.

Leivar, P., Tepperman, J.M., Monte, E., Calderon, R.H., Liu, T.L., and Quail, P.H. (2009). Definition of early transcriptional circuitry involved in light-induced reversal of PIF-imposed repression of photomorphogenesis in young *Arabidopsis* seedlings. Plant Cell **21:** 3535–3553.

Leivar, P., Tepperman, J.M., Cohn, M.M., Monte, E., Al-Sady, B., Erickson, E., and Quail, P.H. (2012). Dynamic antagonism between phytochromes and PIF family basic helix-loop-helix factors induces selective reciprocal responses to light and shade in a rapidly responsive transcriptional network in *Arabidopsis.* Plant Cell **24:** 1398–1419.

Leivar, P., Monte, E., Al-Sady, B., Carle, C., Storer, A., Alonso, J.M., Ecker, J.R., and Quail, P.H. (2008a). The *Arabidopsis* phytochrome-interacting factor PIF7, together with PIF3 and PIF4, regulates responses to prolonged red light by modulating phyB levels. Plant Cell **20:** 337–352.

Leivar, P., Monte, E., Oka, Y., Liu, T., Carle, C., Castillon, A., Huq, E., and Quail, P.H. (2008b). Multiple phytochrome-interacting bHLH transcription factors repress premature seedling photomorphogenesis in darkness. Curr. Biol. **18:** 1815–1823.

Li, L., et al. (2012). Linking photoreceptor excitation to changes in plant architecture. Genes Dev. **26:** 785–790.

Lipford, J.R., and Deshaies, R.J. (2003). Diverse roles for ubiquitin-dependent proteolysis in transcriptional activation. Nat. Cell Biol. **5:** 845–850.

Lipford, J.R., Smith, G.T., Chi, Y., and Deshaies, R.J. (2005). A putative stimulatory role for activator turnover in gene expression. Nature **438:** 113–116.

Lorrain, S., Trevisan, M., Pradervand, S., and Fankhauser, C. (2009). Phytochrome interacting factors 4 and 5 redundantly limit seedling deetiolation in continuous far-red light. Plant J. **60:** 449–461.

Lorrain, S., Allen, T., Duek, P.D., Whitelam, G.C., and Fankhauser, C. (2008). Phytochrome-mediated inhibition of shade avoidance involves degradation of growth-promoting bHLH transcription factors. Plant J. **53:** 312–323.

Luo, Q., Lian, H.L., He, S.B., Li, L., Jia, K.P., and Yang, H.Q. (2014). COP1 and phyB physically Interact with PIL1 to Regulate Its Stability and Photomorphogenic Development in *Arabidopsis.* Plant Cell **26:** 2441–2456.

Ma, L., Li, J., Qu, L., Hager, J., Chen, Z., Zhao, H., and Deng, X.W. (2001). Light control of *Arabidopsis* development entails coordinated regulation of genome expression and cellular pathways. Plant Cell **13:** 2589–2607.

Mitchell, P.J., and Tjian, R. (1989). Transcriptional regulation in mammalian cells by sequence-specific DNA binding proteins. Science **245:** 371–378.

Moon, J., Zhu, L., Shen, H., and Huq, E. (2008). PIF1 directly and indirectly regulates chlorophyll biosynthesis to optimize the greening process in *Arabidopsis.* Proc. Natl. Acad. Sci. USA **105:** 9433–9438.

Muratani, M., and Tansey, W.P. (2003). How the ubiquitin-proteasome system controls transcription. Nat. Rev. Mol. Cell Biol. **4:** 192–201.

Murre, C., et al. (1989). Interactions between heterologous helix-loop-helix proteins generate complexes that bind specifically to a common DNA sequence. Cell **58:** 537–544.

Nagatani, A. (2010). Phytochrome: structural basis for its functions. Curr. Opin. Plant Biol. **13:** 565–570.

Ni, W., Xu, S.L., Chalkley, R.J., Pham, T.N., Guan, S., Maltby, D.A., Burlingame, A.L., Wang, Z.Y., and Quail, P.H. (2013). Multisite light-induced phosphorylation of the transcription factor PIF3 is necessary for both its rapid degradation and concomitant negative

feedback modulation of photoreceptor phyB levels in *Arabidopsis.* Plant Cell **25:** 2679–2698.

Ni, W., Xu, S.L., Tepperman, J.M., Stanley, D.J., Maltby, D.A., Gross, J.D., Burlingame, A.L., Wang, Z.Y., and Quail, P.H. (2014). A mutually assured destruction mechanism attenuates light signaling in *Arabidopsis.* Science **344:** 1160–1164.

Oh, E., Zhu, J.Y., and Wang, Z.Y. (2012). Interaction between BZR1 and PIF4 integrates brassinosteroid and environmental responses. Nat. Cell Biol. **14:** 802–809.

Oh, E., Kim, J., Park, E., Kim, J.I., Kang, C., and Choi, G. (2004). PIL5, a phytochrome-interacting basic helix-loop-helix protein, is a key negative regulator of seed germination in *Arabidopsis thaliana.* Plant Cell **16:** 3045–3058.

Oh, E., Kang, H., Yamaguchi, S., Park, J., Lee, D., Kamiya, Y., and Choi, G. (2009). Genome-wide analysis of genes targeted by PHYTOCHROME INTERACTING FACTOR 3-LIKE5 during seed germination in *Arabidopsis.* Plant Cell **21:** 403–419.

Park, E., Park, J., Kim, J., Nagatani, A., Lagarias, J.C., and Choi, G. (2012). Phytochrome B inhibits binding of phytochrome-interacting factors to their target promoters. Plant J. **72:** 537–546.

Pfalz, J., Liere, K., Kandlbinder, A., Dietz, K.J., and Oelmüller, R. (2006). pTAC2, -6, and -12 are components of the transcriptionally active plastid chromosome that are required for plastid gene expression. Plant Cell **18:** 176–197.

Pfeiffer, A., Shi, H., Tepperman, J.M., Zhang, Y., and Quail, P.H. (2014). Combinatorial complexity in a transcriptionally centered signaling hub in *Arabidopsis.* Mol. Plant **7:** 1598–1618.

Piskacek, S., Gregor, M., Nemethova, M., Grabner, M., Kovarik, P., and Piskacek, M. (2007). Nine-amino-acid transactivation domain: establishment and prediction utilities. Genomics **89:** 756–768.

Ptashne, M. (1988). How eukaryotic transcriptional activators work. Nature **335:** 683–689.

Rausenberger, J., Hussong, A., Kircher, S., Kirchenbauer, D., Timmer, J., Nagy, F., Schäfer, E., and Fleck, C. (2010). An integrative model for phytochrome B mediated photomorphogenesis: from protein dynamics to physiology. PLoS ONE **5:** e10721.

Reid, G., Hübner, M.R., Métivier, R., Brand, H., Denger, S., Manu, D., Beaudouin, J., Ellenberg, J., and Gannon, F. (2003). Cyclic, proteasome-mediated turnover of unliganded and liganded ERalpha on responsive promoters is an integral feature of estrogen signaling. Mol. Cell **11:** 695–707.

Rizzini, L., Favory, J.J., Cloix, C., Faggionato, D., O'Hara, A., Kaiserli, E., Baumeister, R., Schäfer, E., Nagy, F., Jenkins, G.I., and Ulm, R. (2011). Perception of UV-B by the *Arabidopsis* UVR8 protein. Science **332:** 103–106.

Rockwell, N.C., Su, Y.S., and Lagarias, J.C. (2006). Phytochrome structure and signaling mechanisms. Annu. Rev. Plant Biol. **57:** 837–858.

Sadowski, I., Ma, J., Triezenberg, S., and Ptashne, M. (1988). GAL4-VP16 is an unusually potent transcriptional activator. Nature **335:** 563–564.

Salghetti, S.E., Caudy, A.A., Chenoweth, J.G., and Tansey, W.P. (2001). Regulation of transcriptional activation domain function by ubiquitin. Science **293:** 1651–1653.

Salghetti, S.E., Muratani, M., Wijnen, H., Futcher, B., and Tansey, W.P. (2000). Functional overlap of sequences that activate transcription and signal ubiquitin-mediated proteolysis. Proc. Natl. Acad. Sci. USA **97:** 3118–3123.

Schwechheimer, C., Smith, C., and Bevan, M.W. (1998). The activities of acidic and glutamine-rich transcriptional activation domains in plant cells: design of modular transcription factors for high-level expression. Plant Mol. Biol. **36:** 195–204.

Shen, H., Zhu, L., Castillon, A., Majee, M., Downie, B., and Huq, E. (2008). Light-induced phosphorylation and degradation of the negative regulator PHYTOCHROME-INTERACTING FACTOR1 from *Arabidopsis* depend upon its direct physical interactions with photoactivated phytochromes. Plant Cell **20:** 1586–1602.

Shin, J., Kim, K., Kang, H., Zulfugarov, I.S., Bae, G., Lee, C.H., Lee, D., and Choi, G. (2009). Phytochromes promote seedling light responses by inhibiting four negatively-acting phytochrome-interacting factors. Proc. Natl. Acad. Sci. USA **106:** 7660–7665.

Spoel, S.H., Mou, Z., Tada, Y., Spivey, N.W., Genschik, P., and Dong, X. (2009). Proteasome-mediated turnover of the transcription coactivator NPR1 plays dual roles in regulating plant immunity. Cell **137:** 860–872.

Stephenson, P.G., Fankhauser, C., and Terry, M.J. (2009). PIF3 is a repressor of chloroplast development. Proc. Natl. Acad. Sci. USA **106:** 7654–7659.

Tepperman, J.M., Hwang, Y.S., and Quail, P.H. (2006). phyA dominates in transduction of red-light signals to rapidly responding genes at the initiation of *Arabidopsis* seedling de-etiolation. Plant J. **48:** 728–742.

Till, B.J., et al. (2003). Large-scale discovery of induced point mutations with high-throughput TILLING. Genome Res. **13:** 524–530.

Toledo-Ortiz, G., Huq, E., and Quail, P.H. (2003). The *Arabidopsis* basic/helix-loop-helix transcription factor family. Plant Cell **15:** 1749–1770.

Toledo-Ortiz, G., Huq, E., and Rodríguez-Concepción, M. (2010). Direct regulation of phytoene synthase gene expression and carotenoid biosynthesis by phytochrome-interacting factors. Proc. Natl. Acad. Sci. USA **107:** 11626–11631.

Uesugi, M., Nyanguile, O., Lu, H., Levine, A.J., and Verdine, G.L. (1997). Induced alpha helix in the VP16 activation domain upon binding to a human TAF. Science **277:** 1310–1313.

Van Buskirk, E.K., Decker, P.V., and Chen, M. (2012). Photobodies in light signaling. Plant Physiol. **158:** 52–60.

Van Buskirk, E.K., Reddy, A.K., Nagatani, A., and Chen, M. (2014). Photobody localization of phytochrome B is tightly correlated with prolonged and light-dependent inhibition of hypocotyl elongation in the dark. Plant Physiol. **165:** 595–607.

Vojnic, E., Mourão, A., Seizl, M., Simon, B., Wenzeck, L., Larivière, L., Baumli, S., Baumgart, K., Meisterernst, M., Sattler, M., and Cramer, P. (2011). Structure and VP16 binding of the Mediator Med25 activator interaction domain. Nat. Struct. Mol. Biol. **18:** 404–409.

von der Lehr, N., et al. (2003). The F-box protein Skp2 participates in c-Myc proteosomal degradation and acts as a cofactor for c-Myc-regulated transcription. Mol. Cell **11:** 1189–1200.

Williams-Carrier, R., Zoschke, R., Belcher, S., Pfalz, J., and Barkan, A. (2014). A major role for the plastid-encoded RNA polymerase complex in the expression of plastid transfer RNAs. Plant Physiol. **164:** 239–248.

Wu, D., Hu, Q., Yan, Z., Chen, W., Yan, C., Huang, X., Zhang, J., Yang, P., Deng, H., Wang, J., Deng, X., and Shi, Y. (2012). Structural basis of ultraviolet-B perception by UVR8. Nature **484:** 214–219.

Xu, X., Paik, I., Zhu, L., Bu, Q., Huang, X., Deng, X.W., and Huq, E. (2014). PHYTOCHROME INTERACTING FACTOR1 enhances the E3 ligase activity of CONSTITUTIVE PHOTOMORPHOGENIC1 to synergistically repress photomorphogenesis in *Arabidopsis.* Plant Cell **26:** 1992–2006.

Yamaguchi, R., Nakamura, M., Mochizuki, N., Kay, S.A., and Nagatani, A. (1999). Light-dependent translocation of a phytochrome B-GFP fusion protein to the nucleus in transgenic *Arabidopsis.* J. Cell Biol. **145:** 437–445.

Zhai, Q., Yan, L., Tan, D., Chen, R., Sun, J., Gao, L., Dong, M.Q., Wang, Y., and Li, C. (2013). Phosphorylation-coupled proteolysis of the transcription factor MYC2 is important for jasmonate-signaled plant immunity. PLoS Genet. **9:** e1003422.

Zhang, Y., Mayba, O., Pfeiffer, A., Shi, H., Tepperman, J.M., Speed, T.P., and Quail, P.H. (2013). A quartet of PIF bHLH factors provides a transcriptionally centered signaling hub that regulates seedling morphogenesis through differential expression-patterning of shared target genes in *Arabidopsis.* PLoS Genet. **9:** e1003244.